

Modeling Agricultural Nonpoint Source Pollution Using a Geographic Information System Approach

Lisa A. Emili · Richard P. Greene

Received: 15 December 2010 / Accepted: 14 August 2012 / Published online: 16 September 2012
© Springer Science+Business Media, LLC 2012

Abstract Agricultural non-point source (NPS) pollution, primarily sediment and nutrients, is the leading source of water-quality impacts to surface waters in North America. The overall goal of this study was to develop geographic information system (GIS) protocols to facilitate the spatial and temporal modeling of changes in soils, hydrology, and land-cover change at the watershed scale. In the first part of this article, we describe the use of GIS to spatially integrate watershed scale data on soil erodibility, land use, and runoff for the assessment of potential source areas within an intensively agricultural watershed. The agricultural non-point source pollution (AGNPS) model was used in the Muddy Creek, Ontario, watershed to evaluate the effectiveness of management strategies in decreasing sediment and nutrient [phosphorus (P)] pollution. This analysis was accompanied by the measurement of water-quality parameters (dissolved oxygen, pH, hardness, alkalinity, and turbidity) as well as sediment and P loadings to the creek. Practices aimed at increasing year-round soil cover would be most effective in decreasing sediment and P losses in this watershed. In the second part of this article, we describe a method for characterizing land-cover change in a dynamic urban fringe watershed. The GIS method we developed for the Blackberry Creek, Illinois, watershed will allow us to better account for temporal changes in land use, specifically corn and soybean cover, on an annual basis and to improve on the modeling of watershed processes shown for the

Muddy Creek watershed. Our model can be used at different levels of planning with minimal data preprocessing, easily accessible data, and adjustable output scales.

Keywords AGNPS · Soil erosion · Watershed assessment · Non-point source · Land use

Introduction

Agricultural non-point source (NPS) pollution is the leading source of water-quality impacts to surface water in North America (The Conference Board of Canada 2010; United States Environmental Protection Agency 2002; David and Gentry 2000). The primary pollutants are eroded sediment and fertilizer-derived nutrients, particularly phosphorus (P). Agricultural lands constitute 50 % of land use in the United States, and with a projected doubling of agricultural yield by 2050 (United States Department of Agriculture 2009), agronomic systems may become increasingly dependent on fertilizer and pesticide inputs. The long-term consequences of these increases are largely unknown (United States Department of Agriculture 2009).

Although inputs of P are essential for profitable crop and livestock agriculture, they accelerate eutrophication of receiving waters (Sharpley and others 2003). This cultural eutrophication results in rapid increases in the rate of biological production and a wide range of undesirable water-quality changes in freshwater and marine ecosystems (Ghadouani and Coggins 2011; National Research Council 2000). Communities are burdened with increased costs of water treatment and decreased recreational and tourism uses associated with algal blooms (Hoagland and others 2002).

A significant portion (≤ 80 %) of P transported in runoff to receiving water is transported as sediment-bound P

L. A. Emili (✉)
Division of Mathematics and Natural Sciences, Penn State
Altoona, 3000 Ivyside Park, Altoona, PA 16601, USA
e-mail: lae18@psu.edu

R. P. Greene
Department of Geography, Northern Illinois University,
231 North Annie Glidden Road, DeKalb, IL 60115, USA
e-mail: rgreene@niu.edu

during storm events (Sharpley and others 1992). P loadings, therefore, are a function of the same factors affecting soil erosion. Management practices to decrease sediment-associated P loss in agricultural runoff must be twofold: source and transport control strategies. The efficiency of use, e.g., fertilizer-application rates, must be improved. Conservation practices, such as decreased tillage, cover crops, and buffer strips, must be targeted to areas where P availability, soil erosion potential, and surface runoff is high (Sharpley 1995). The determination of priority source areas (PSAs) (Shen and others 2011) of NPS pollution is essential for risk assessment and the effective implementation of best-management practices (BMPs) aimed at decreasing the input of pollutants to surface waters.

This article focuses on two pilot examples of geographic information system (GIS) methods to examine the relative importance of land use change on stream water quality and NPS pollution potential in agricultural watersheds. Distributed-parameter NPS pollution models have been useful tools in producing comprehensive watershed models able to simulate the effects of alternative control measures (Wu and others 2005). We use a modified version of one such model, the AGNPS pollution model, developed by the USDA's Agricultural Research Service (Young and others 1994), to investigate alternative management strategies in a small watershed (Muddy Creek) in southwestern Ontario, Canada. An understanding of the dynamics of land use change and water quality under a range of scenarios is essential for sustainable and adaptive water resources management (Praskievicz and Chang 2011).

Increasingly, agricultural watersheds are experiencing urban development pressures (Barco and others 2008). The spatial patterns of urban development have a significant impact on the timing and magnitude of runoff and water quality (Randhir and Hawes 2009). We built a GIS-based model to examine long- and short-term changes in land-cover in an urban fringe watershed (Blackberry Creek) located in northeastern Illinois.

The overall goal of this study was to develop GIS protocols to facilitate the spatial and temporal modeling of changes in soils, hydrology, and land-cover change in agricultural watersheds. We develop and apply methods that integrate remotely sensed data, GIS-based data, and distributed-parameter model output data to assess the potential for sediment and nutrient runoff in the study watersheds.

The specific objectives of this study were to use GIS as follows:

1. To generate GIS layers for the hydrophysical resources of the Muddy Creek watershed;
2. to spatially represent AGNPS model results and potential sources areas of NPS pollution in the Muddy Creek watershed; and
3. to characterize land-cover change for the Blackberry Creek watershed to better account for land use change as well as corn and soybean crop coverage.

Muddy Creek Watershed

Study Area

The study site is located along the northern shore of Lake Erie in Southwestern Ontario, Canada (Fig. 1). Muddy Creek is a Lake Erie tributary that flows south through the Muddy Creek wetland into Wheatley Harbour (Fig. 2). In the upper reaches, the natural drainage has been modified by municipal drains, open ditches, and dredge cuts. These modifications serve as outlets for tile drains and may accelerate the rate of subsurface runoff during spring thaw and storm events (Huber 1992).

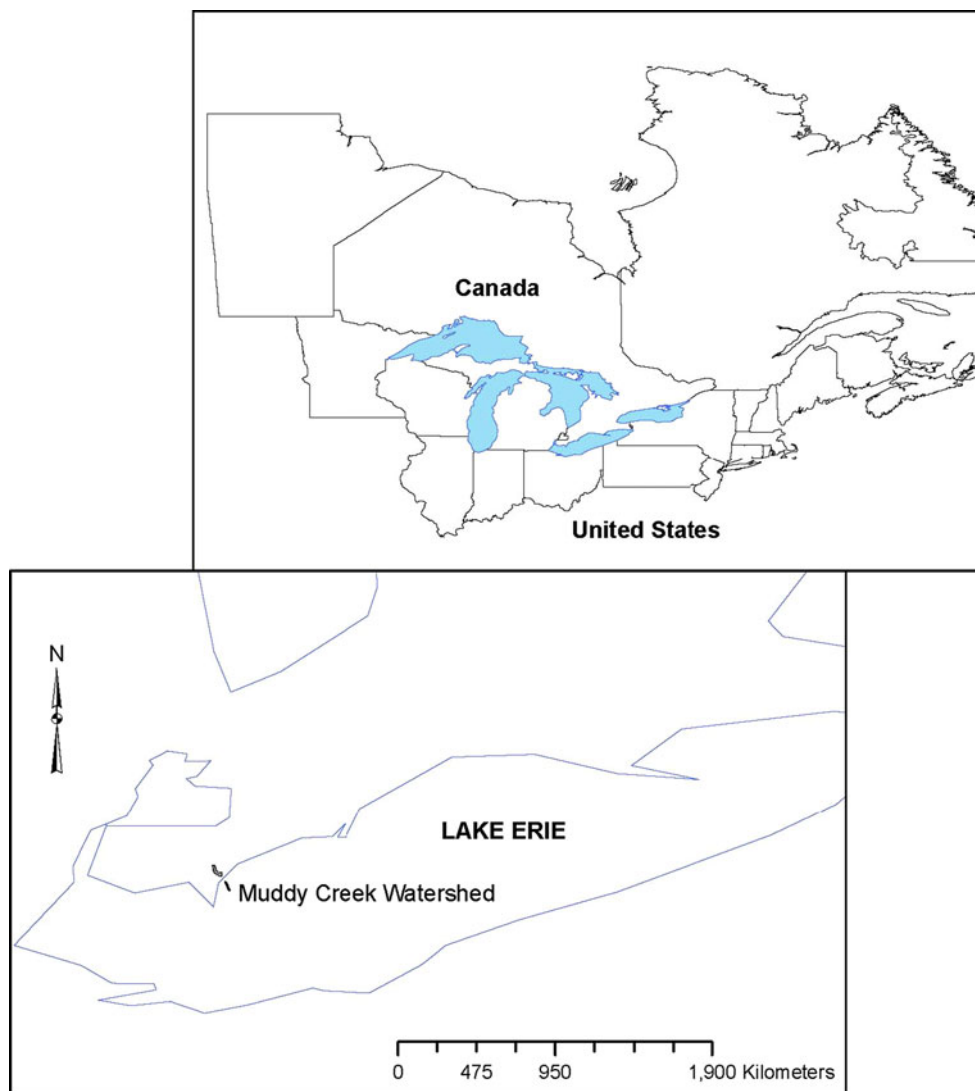
The watershed (8.75 km²) is under predominantly agricultural land use, with <8 % of the land under non-agricultural uses. Crop types consist of mainly market gardening and cash crops with corn, soybeans, winter wheat, and tomatoes dominating (Fig. 3). Land use changes to a combination of industrial and commercial at the adjoining harbor, where commercial fisheries and a fish- and food-processing plant are located. Sandy beaches flanking the harbor support recreational facilities, such as a park, camp grounds, and cottages.

Approximately 90 % of the wetland consists of an embayment of open water with shoreline vegetation of cattail marshes and lowland swamp forests of Silver Maple. The marshes are an important staging area for migratory waterfowl, and the wetland system provides habitat for provincially significant flora and fauna.

The harbor was previously designated as an area of concern (AOC) due to a history of oxygen depletion, increased bacterial levels, nutrient enrichment, and organic contamination of harbor sediments (Huber 1992). After several phases of remedial action, the AOC designation has been lifted. The improvements to water quality have largely been the result of improved wastewater treatment by the fish- and food-processing plant and sewage treatment by the local township (Environment Canada 2010a).

The average daily temperature is 9.2 °C, with July being the warmest month (daily mean 22.3 °C) and January the coldest (daily mean −4.5 °C). The average length of the growing season is 216 days with an average frost-free period of 165–169 days. Mean annual rainfall is 809.3 mm, 42 % occurring in June through September. The greatest daily maximum rainfall occurs from July to September (111.6, 91.4, and 106.4 mm, respectively; Environment Canada 2010b).

Fig. 1 Location of the Muddy Creek watershed within the Great Lakes Basin



The watershed drains a smooth clay veneer till plain with scattered sandy knolls. The underlying bedrock comprises Devonian limestone, dolomite, and gypsum. Overlying soils (Fig. 4) in the upper reaches are poorly drained Brookston clay sands intermixed with Brookston clays classified as clayey, mixed, and mesic Typic Argiaquolls. Two lenses of Berrien sandy loams (sandy, mixed, and mesic Paleudults) are found in the upper and middle sections of the watershed. These soils are imperfectly drained. Well drained Plainfield sands (mixed and mesic Typic Udipsamments) occur as a sand ridge running northeast/southwest across the middle of the watershed. In the lower reaches, drainage is poor on the heavily textured Brookston clays. Soils immediately around the wetlands and harbor are variably drained bottom lands subject to flooding. The topography is generally flat.

Research Approach

To develop a GIS protocol for the modeling of spatial-temporal changes in land use and associated sediment- and P-pollution potential at the watershed scale, we needed a comprehensive data set for land use and farming practices for our study watershed. Furthermore, we needed a comprehensive data set of sediment and P loadings for model verification. We used an unpublished historical data set collected by the first author (L. A. E.) from which we selected all resource data and GIS layers appropriate for that time period.

Data were derived from a combination of GIS methods (using ArcInfo 10.0 ESRI Redlands, California) and topographic maps because many of the available GIS layers for the study area were not at the spatial resolution needed and/or did not possess attribute data of adequate

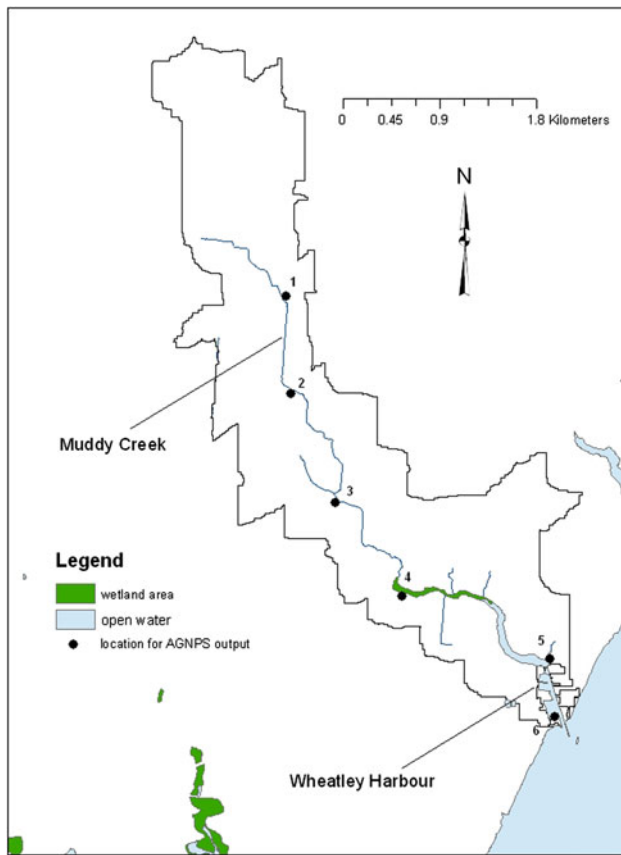


Fig. 2 Muddy Creek watershed with wetland areas and water-quality sampling stations/AGNPS model output locations

detail or delineation. GIS spatial techniques were used to generate terrain based layers for the Muddy Creek watershed. Specifically, digital elevation models (DEMs) (Ontario Ministry of Natural Resources 2006) were used to estimate topographical and hydrological attributes for the determination of slope, drainage/streamflow, and watershed boundaries (Fig. 5). The AGNPS model was initially run without the use of an ArcGIS interface. ArcInfo was then used to overlay and populate the existing grid with model output data to facilitate spatial analysis and representation.

Water Sample Collection and Analytical Methods

Six sampling stations were established along Muddy Creek (Fig. 2). Stations 1 through 4 drain the primarily agricultural portion of the watershed, with station 4 being located adjacent to the riparian wetland. Stations 5 and 6 are located within the harbor. Samples were taken bimonthly, with increased frequency during rain events, from April to November 1993. At each station, pH was measured using an Oaklon microprocessor-based pH tester with automatic temperature compensation calibrated to pH 4 and 7 (± 0.1

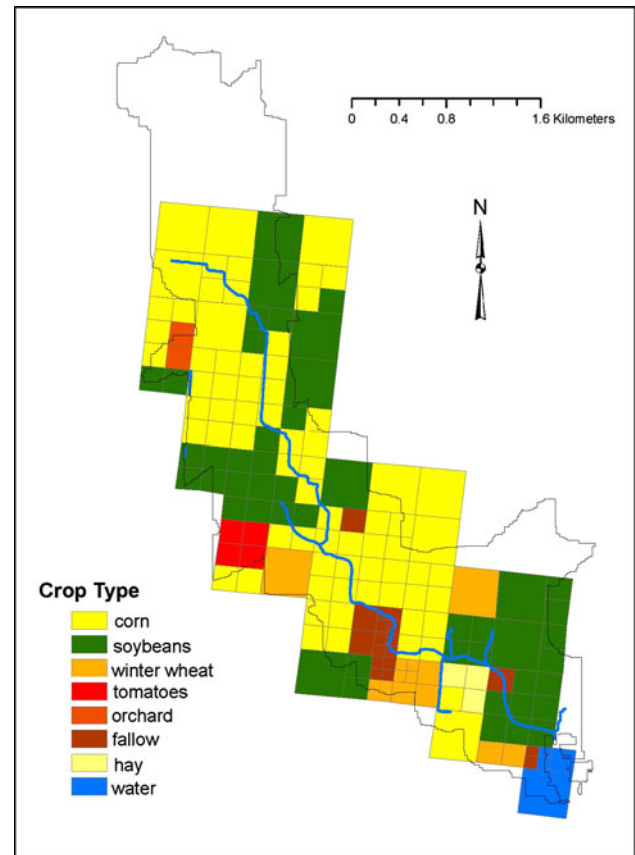


Fig. 3 Crop types in the Muddy Creek watershed displayed as AGNPS model grid input

pH). Dissolved oxygen concentration (DO) and surface water temperature were determined using a YSI Model 58 DO meter calibrated to local barometric pressure. Where depth and flow conditions permitted, a Teledyne Gurley velocity meter was used to measure stream flow.

Surficial sediment samples were collected at five sampling stations using a Petite-Ponar grab sampler (6 × 6 cm). Each sample was homogenized by hand by mixing with a prewashed (pesticide-grade hexane) spoon in a prewashed 2-L glass container (also prewashed). Homogenized samples were collected into plastic ointment jars for freeze-drying and subsequent determination of particle-size distribution and sediment geochemistry. Particle-size distribution was determined using sieving and sedigraph methods (Duncan and LaHaie 1979) at the sedimentology laboratory at the National Water Research Institute (NWRI) of Canada in Burlington, Ontario. The analysis of sediment samples for the determination of major elements was performed by inductively coupled plasma–atomic emission spectroscopy with a multichannel Jarrell-Ash AtomComp 1100. Samples for the determination of major elements (silicon, aluminum [Al], calcium [Ca], magnesium [Mg], potassium, sodium, P, Ti, iron, and

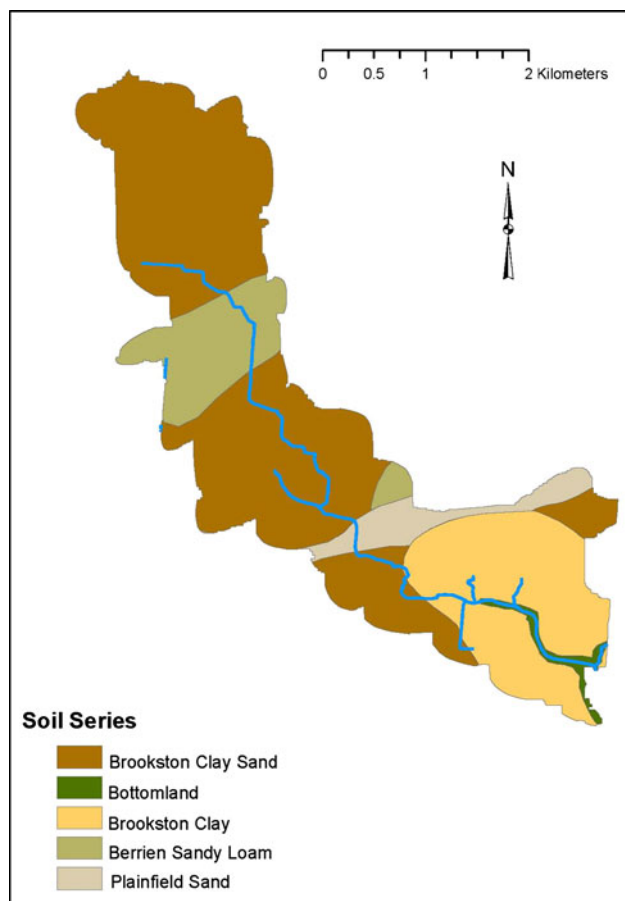


Fig. 4 Soil series of the Muddy Creek watershed

manganese) were ground before analysis. Approximately 0.100 g of the sample was mixed with 0.8 g of Spectroflux 100 B (4:1 lithium meta- and tetraborate) in a graphite crucible. The molten fusion mixture was poured into a container and dissolved with aqua regia. Measurements of the elemental concentrations were performed using a multichannel analyzer.

Two sediment cores were taken at station 4 using a modified hand-operated Kajak-Brinkhurst corer of 6.6 cm diameter. The sediment cores were subsampled vertically into 1-cm sections using a stainless steel slicer and knife. Each subsection from the first core was freeze-dried, homogenized by sieving through a 20 mesh-size sieve, and used in the determination of particle-size distribution and sediment geochemistry (per the method described previously). Subsections from the second core were stored in wet plastic vials for sediment dating. These latter subsections were analyzed by the Paleoenvironmental Research Laboratory at the NWRI for polonium activity for further dating using the lead (Pb)-210 (^{210}Pb) method (Turner 1994).

At each station, a grab sample of water was collected in a 1-L polyethylene bottle for the determination of the

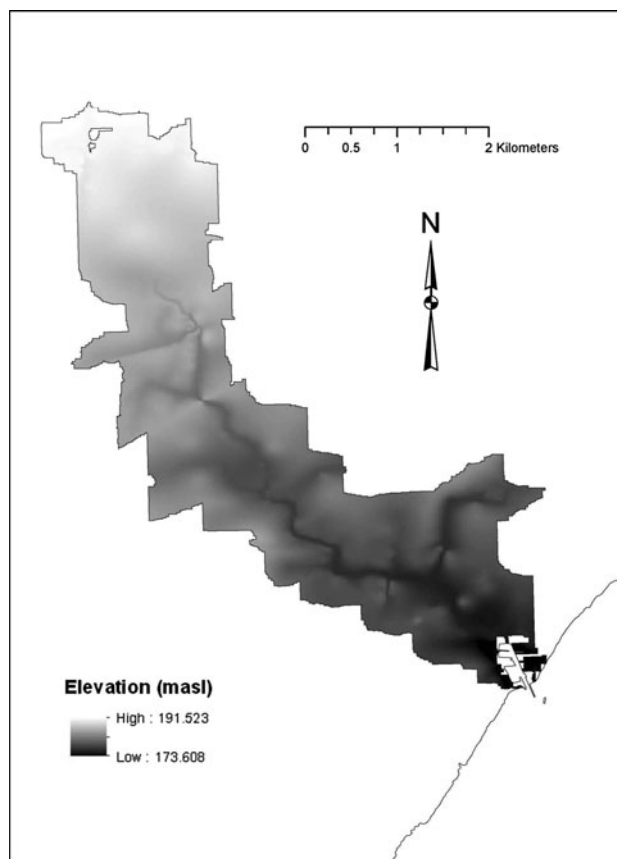


Fig. 5 DEM for the Muddy Creek watershed (Provincial DEM v200, 10-m resolution UTM Zone 17)

concentrations of suspended particulate matter (SPM) by centrifugation and evaporation. Samples were centrifuged on-site by a Westfalia continuous-flow separator at an average rate of 4 L/min and a running time of 5 min. The centrifuge bowls were removed and scrubbed with a plastic cleaning brush and rinsed into a 2-L polyethylene bottle. Any remaining water in the centrifuge bowls was also decanted into the 2-L bottle. Samples were transferred from the 2-L bottles to 1-L preweighed containers. The sample bottles and lids were rinsed with distilled water, and the rinsings were collected with the original sample. The containers were placed in a drying oven at temperature of 38–43 °C and allowed to evaporate to dryness. The containers were cooled to room temperature and weighed.

Water samples were also collected into 500-mL polyethylene bottles for the determination of alkalinity, turbidity, hardness, and concentrations of Ca and Mg. Quantitative determination of these parameters was performed at the National Laboratory for Environmental Testing of the NWRI of Canada. Water hardness was determined by the summation of concentrations of Ca and Mg as determined by atomic absorption spectroscopy. Alkalinity was expressed as the equivalent of calcium carbonate (CaCO_3). CaCO_3 was dissolved in deionized

distilled water and then diluted to volume with the same solution. Alkalinity was then determined by electrometric titration with a standard solution of strong acid or base. Turbidity was determined by comparing the intensity of light scattered by the sample with a standard reference (formazin polymer) under the same light conditions.

Samples for the determination of dissolved organic carbon (DOC) and total filtered and unfiltered P (TP–FP and TP–UF, respectively) were collected in glass jars and acidified with 1 mL 30 % sulfuric acid. TP samples were filtered on-site using a portable stainless steel Fujikin positive-pressure filtration system. The reservoir chamber and filter holder had been prewashed with 1 N nitric acid rinsed with distilled water. A pressure of 103.3 kPa nitrogen was applied. Cellulose nitrate filters (142-mm diameter, 0.45- μ m pore size) with glass fiber prefilters were used. All samples were stored at 4 °C until analysis.

DOC was measured by high-temperature combustion using a Dohrmann DC-190 high-temperature total carbon (C) analyzer (0.5 mg/L SEM) at the National Laboratory for Environmental Testing of the NWRI. Soluble (dissolved) and total P levels were determined using a colorimetric method. The organic matter in the sample was destroyed by digestion with a mixture of sulfuric acid and persulfate during which the organic P is released as phosphate. The acid digestion also hydrolyzes polyphosphates to orthophosphates. The orthophosphate was then reacted with ammonium molybdate to form heteropoly phosphomolybdic acid, which was reduced using stannous chloride in an aqueous sulfuric acid medium to form molybdenum (Mo) blue. The Mo blue color was measured using a Technicon Autoanalyzer unit with colorimeter (50 mm flow cell and 660 nm filters) set at a wavelength of 660 nm. Rainfall was recorded (May through September) using a polyethylene storage rain gauge with an aperture of 41.5 cm² positioned 45 cm above the ground surface 300 m west of station 1.

Spatial Modeling: AGNPS Model Inputs

The AGNPS model is a single event, basin-scale model that operates on a grid (cell) basis (Young and others 1994). Each cell homogeneously represents the landscape within the respective cell boundary. A cell size of 16.2 ha was selected to match the size of land ownership parcels. Basic model components include hydrology, erosion, sediment transport, and chemical transport.

Each cell is characterized by 22 input parameters, including cell number (54 total for the Muddy Creek watershed), division, receiving cell number, aspect/flow direction, curve number (CN), land slope, land slope shape factor, field-slope length, channel slope, channel side slope, Manning's roughness coefficient (*n*-factor), soil erodibility

factor (*K*-factor), cropping factor (*C*-factor), conservation-practice factor (*P*-factor), surface condition constant, soil texture, fertilizer level, fertilizer-availability (incorporation) factor, point source indicator, gully source level, chemical oxygen demand (COD) factor, impoundment factor, and channel indicator. Standard values for the model inputs were used as indicated by the user's guide (Young and others 1994). Where more than one land use condition existed within a cell, a weighted average was used. Where nonuniform conditions existed within a cell for the following input parameters—CN, channel slope, channel sideslope, *n*-factor, *K*-factor, *C*-factor, *P*-factor, surface condition constant, fertilizer-availability factor, and COD—the predominant condition in the cell was used. COD is a measure of the oxygen required to oxidize organic and oxidizable inorganic compounds in water and is often used as an indicator of the degree of water pollution by organic material (Wang and others 2011).

Slope aspect, slope length, slope shape, channel slope and channel side slope for the Muddy Creek watershed were based on topographic map interpretation. Seasonal values for spring, summer, and fall were used for the *n*-factor (=0.039, 0.025, 0.039) and the *C*-factor (=0.35, 0.40, 0.29, respectively) (Young and others 1994). There were no point sources, impoundments, or significant gully inputs to the creek.

Input cell data for fertilization level and availability were obtained from existing records, visual reconnaissance, and a farmer questionnaire. Field reconnaissance consisted of manual rainfall data collection as well as measurement of basic meteorologic (temperature and wind) and water conditions (stream velocity, depth, and temperature). In-person interviews were conducted throughout the sampling season. Survey questions included crop-management practices (e.g., seed date, harvest date, rotation, treatment, and tillage) and fertilizer and pesticide application (e.g., type, rate, and timing). The survey response rate was 76 %. Regarding cells for which there were no survey response data, recommended fertilization levels (Ontario Ministry of Agriculture, Food and Rural Affairs 1994) according to crop type were used. In addition, where possible, the fertilizer-availability factor was based on field observation of tillage practices; for unknown conditions, an availability factor of 50 % was used.

Watershed level inputs for total precipitation of the storm events May 15, July 8, and November 1, 1993, were 27.9, 55.9, and 17.8 mm, respectively. Energy intensity for these same three events was determined as 3.4, 18.0, and 4.0 according to Rudra and others (1986). Assigned CN values were adjusted for individual storms depending on the antecedent moisture condition (AMC) before each storm event in the AGNPS input file. The AMC of a watershed was determined by the 5-day antecedent rainfall amount (Soil Conservation Service 1968).

Of the AGNPS model (version 5.00; Young and others 1994) runs, three dates were selected as being representative of crop-stage period for a growing season (May 15 [spring] = spring conditions, crops planted, and fertilizers applied; July 8 [summer] = midseason conditions; November 1 [fall] = completion of growing season, crops harvested, winter wheat planted) under four scenarios: existing conditions, worst case conditions (summer fallow), alternative management option 1 (winter wheat for year-round soil cover), and alternative management option 2 (combined use of no-till on clay soils and maintenance of a corn residue). Output was generated at the watershed outlet and at six locations along Muddy Creek (Fig. 2).

Although fallow conditions are not standard practice, in mixed use and particularly in agricultural watersheds experiencing urban development, previously tilled and cultivated agricultural land is unused or left fallow between the time that it has been purchased for development and the onset of construction (Manonmani 2010). In some communities, there is a requirement that agricultural land must be left fallow for a designated period before urban development (Manonmani 2010). In Illinois specifically, the economic downturn has resulted in the delay or termination of subdivision construction, leaving former agricultural land at varying stages of development where the land may have been cleared and/or utilities or roadways installed.

Data Acquisition and Development of GIS Layers

The provincial boundary, municipal boundaries, hydrography (water lines and polygons), quaternary watershed boundaries, and soil survey layers were acquired through the Land Information Ontario (LIO) Geospatial Warehouse Data Subscription Service (Ontario Ministry of Natural Resources 2010). Wetland area was derived as a subset of the hydrography.

Multiple 10-m DEMs for the Province of Ontario were also acquired from the LIO warehouse (Ontario Ministry of Natural Resources 2006), and the watershed boundary was used to delineate extent. The watershed boundary was delineated using the Spatial Analyst hydrology tools in ArcInfo 10.0. Any internal boundaries were eliminated by converting the raster layer to polygons and dissolving.

The AGNPS model operates on a grid (cell) basis. Input and output data are routed through the grid of cells representing the watershed area. A scanned version of the model output grid was imported into ArcMap, georeferenced, and rectified (bilinear interpolation). The extent of the grid was digitized as a new feature. The internal cell divisions were created using the Cut Polygon feature in the editing mode.

Information on land use and farming practices, such as crop type, crop dates, tillage techniques, and fertilizer-applications, was obtained through field reconnaissance and interviews with local farmers as detailed previously. These input data were used to produce the model output presented later in the text. Fields for crop type, soil erodibility, fertilizer-availability, and sediment P output data were added to the model attribute table, and the grid cells were populated for these values. Each cell was then selected and the information added as an integer representative of specific crop type, erodibility (K), and fertilizer-availability.

The GIS soil layer is based on original soil maps and surveys performed in 1949 and digitized by the Ontario Ministry of Agriculture, Food and Rural Affairs (2004). Based on aerial photos, topographic maps, and field study, the bottomland soil boundary was determined to be inaccurate. ArcInfo 10.0 editing tools were used to reposition the vertices of the boundary line and topological rules (e.g., polygons must not overlap and must not have gaps) were used to maintain data integrity. All layers were projected to Universal Transverse Mercator Zone 17, NAD 1983, for further analyses.

Table 1 pH values (± 0.1 pH accuracy) for Muddy Creek

Sampling dates	Station 1	Station 2	Station 3	Station 4	Station 5	Station 6
19–21 April	7.6	–	7.8	7.6	–	8.1
25–27 May	7.5	–	7.8	7.5	7.9	8.1
7–9 June	7.3	7.1	7.4	7.4	7.6	8.3
28–29 June	7.5	7.2	7.6	7.0	7.6	8.3
12–14 July	8.2	7.7	7.6	7.7	7.8	8.2
27–30 July	7.9	7.7	7.6	8.4	7.8	8.2
9–10 August	7.6	8.2	8.6	7.9	6.9	7.1
28–30 August	–	–	7.6	7.7	7.6	7.8
28–29 September	7.4	7.4	7.2	7.8	7.4	7.9
3–4 November	5.2	5.2	5.5	–	7.1	7.1

Table 2 DO (mg/L) for Muddy Creek

Sampling dates	Station 1	Station 2	Station 3	Station 4	Station 5	Station 6
19–21 April	11.55	–	11.05	–	7.13	8.13
25–27 May	5.85	–	7.93	9.93	8.87	8.80
7–9 June	7.38	7.40	7.32	6.47	4.14	8.52
28–29 June	9.50	6.07	7.09	4.21	5.40	8.47
12–14 July	8.35	5.31	4.12	4.38	6.65	6.59
27–30 July	4.80	–	6.80	13.52	6.07	5.40
9–10 August	2.45	9.53	18.86	5.37	8.49	7.72
28–30 August	–	–	2.68	8.59	4.84	4.86
28–29 September	7.39	8.72	5.49	8.83	7.98	9.71
3–4 November	8.80	7.03	3.45	9.80	8.34	9.55

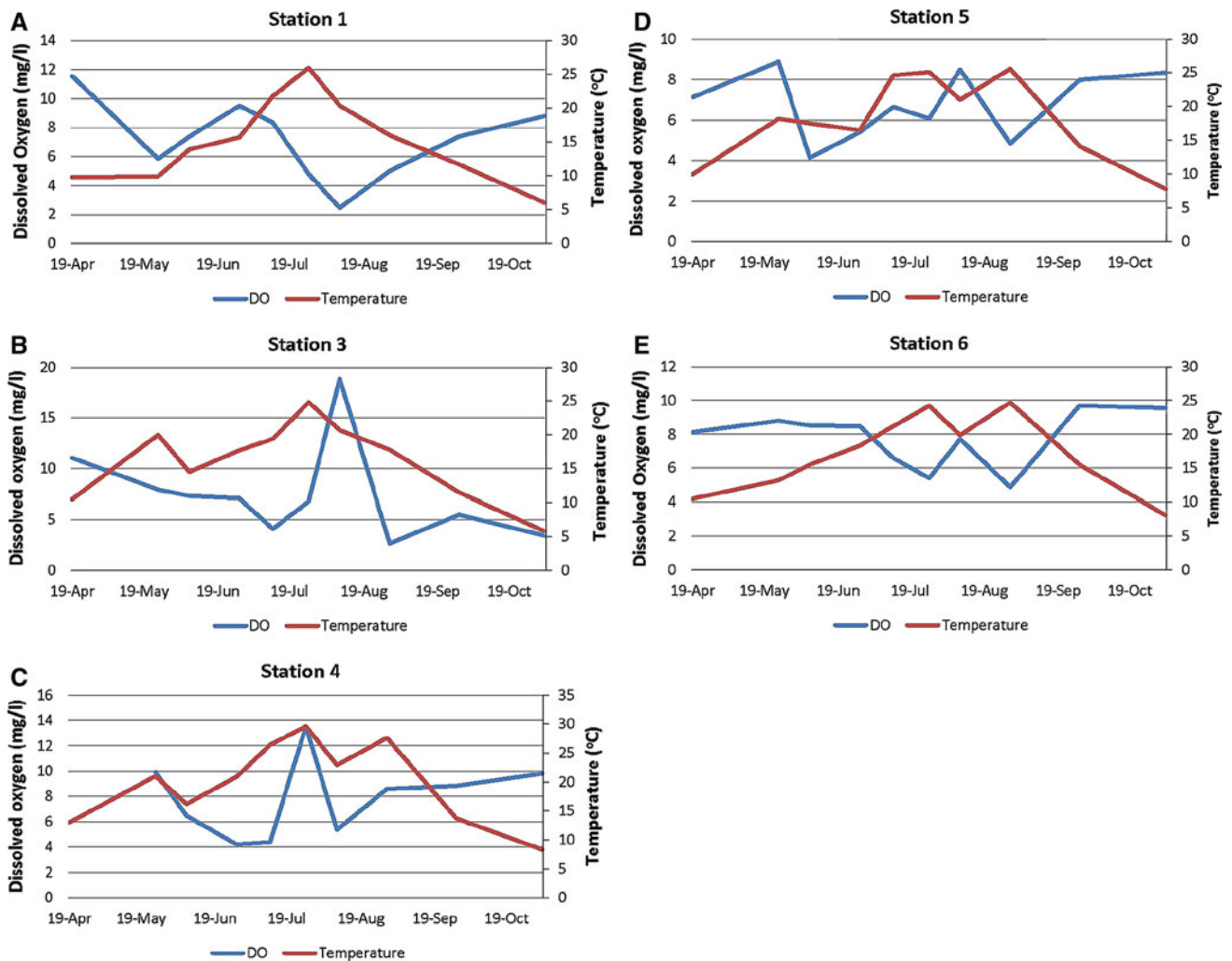


Fig. 6 DO (mg/L) concentrations versus surface water temperature (°C) for stations 1, 3, and 4 through 6 at Muddy Creek watershed

Water Quality

Several water-quality parameters were investigated in the Muddy Creek watershed. These parameters are

interdependent and indicative of the pollution potential of the watershed. The pH values (Table 1) fell within the range (6.5–9.0) recommended for the protection of fresh-water aquatic life (Canadian Council of Ministers of the

Table 3 DOC (mg/L) in Muddy Creek

Sampling date	Station 1	Station 2	Station 3	Station 4	Station 5	Station 6
10 February	2.0	–	3.4	5.5	5.7	3.5
20 April	3.4	–	7.1	–	7.3	6.1
26 May	8.3	10.1	12.5	68.8	4.8	–
27 May	–	–	–	71.5	–	4.7
7 June	11.8	12.2	10.2	9.2	7.2	4.0
28 June	9.2	8.5	8.1	–	–	–
29 June	9.3	–	8.0	8.3	4.3	3.3
30 June	7.6	–	8.2	–	–	–
12 July	6.3	–	–	–	–	–
13 July	7.1	–	6.3	8.7	4.1	22.1
14 July	7.6	–	8.3	–	3.1	–
27 July	9.1	–	14.1	11.5	4.3	2.4
28 July	11.5	12.1	16.7	–	–	–
10 August	9.9	14.4	17.1	10.4	4.1	2.6
30 August	–	19.9	19.9	12.0	3.7	2.4
28 September	8.5	–	9.5	6.8	4.9	3.1

Environment 2011) with the exception of stations 1–3 in November.

Dissolved Oxygen

The DO content of surface water is an indicator of a water body's ability to support aquatic organisms; values <4.0 mg/L threaten aquatic life (Canadian Council of Ministers of the Environment 2011). DO concentrations in Muddy Creek (Table 2) were at or lower than this guideline concentration throughout the summer months, particularly in mid-July and late August through early September. These low concentrations corresponded to late summer and early fall dieback and decomposition of algae. The maximum DO concentrations of 13.52 mg/L (station 4) and 18.86 mg/L (station 3) occurred in late July and early August, respectively, and were associated with an increase in photosynthetic oxygen from mid-summer algal blooms.

Station 6 exhibited an inverse relationship between DO and water temperature throughout the entire sampling season (Fig. 6e). Stations 1 through 5 exhibited varying trends. The water at these stations is shallow, wind-mixed, and influenced by air temperature. An increase in water depth at stations 4 through 6 appeared to dampen the effect of air temperature on water temperature.

In general, for stations 1 through 5, DO and water temperature exhibited opposite trends in mid- to late June and showed similar trends in spring (Fig. 6a, d). These trends indicated an increase in light and temperature conditions favoring algal growth and increased photosynthetic oxygen, with an early summer dieback preceding a second

mid- to late summer algal bloom and decomposition in late summer through early fall.

Dissolved Organic Carbon

At all stations, with the exception of station 3, spring concentrations of DOC (Table 3) were greater than those in the late summer peak. At station 4, high concentrations of DOC in spring (33 mg/L greater than the next closest high concentration) were observed compared with the other stations. The peak in DOC in May at this station may be a measurement error due to the large amount of colloidal material that bypassed the centrifuge used to separate SPM from the water. The lowest concentrations of DOC for stations in the upper watershed occurred in February, whereas minimum DOC concentrations for lower watershed stations occurred in mid-July. Low DOC may be attributed to one or all of the following conditions: stagnant water, decomposition of organic matter, and low water levels. DOC concentrations peaked in early June and late July or August for stations 1 through 4. DOC at stations 5 and 6 peaked in spring and decreased throughout fall. Light conditions in the spring may have favored increased productivity despite lower water temperatures.

Turbidity

Turbidity is a measure of water clarity and can indicate increased erosion and/or algal blooms. According to drinking-water standards (Canadian Council of Ministers of the Environment 2011), turbidity in Muddy Creek was excessive. For stations 1 through 5, peaks in turbidity

Table 4 Turbidity concentrations (JTU) in Muddy Creek

Sampling date	Station 1	Station 2	Station 3	Station 4	Station 5	Station 6
10 February	7.3	–	0.27	4.6	0.85	7.6
20 April	300	–	150	–	50	22.4
26 May	235	300	18.5	210	45	–
27 May	–	–	–	17.2	–	7.6
8 June	275	300	660	750	–	21
9 June	240	–	195	–	412	–
28 June	800	500	1,175	–	–	–
29 June	31	–	41	590	215	4.3
30 June	288	–	39.5	–	–	–
12 July	4.6	4.2	–	–	–	–
13 July	0.45	–	9.0	16	3.1	–
14 July	6.25	–	9.0	–	7.4	19.5
27 July	–	–	32.5	10	40	21.5
28 July	33.5	225	40	–	–	–
10 August	–	225	37.5	375	48.5	20
31 August	–	–	143	380	250	8.7
1 September	–	975	450	–	–	–
28 September	<0.05	8.7	34	42	37.5	21.5
3 November	6,500	25	–	160	150	87

Table 5 SPM concentrations (mg/L) in Muddy Creek

Sampling date(s)	Station 1	Station 3	Station 4	Station 5	Station 6
10 February	9.3	5.7	8.4	34	22
20 April	126	92	–	80	35
26–27 May	137	29	139	68	34
8–9 June	110	127	305	347	29
28–30 June	506	671	229	92	20
12–14 July	63	42	165	84	29
26–28 July	–	–	156	68	24
9–11 August	–	118	189	90	26
30–31 August	–	163	155	47	27
27–28 September	–	32	–	101	24
2–4 November	881	46	89	190	102

(Table 4) occurred in spring, early summer, and late summer. Summer increases in turbidity were greater than spring turbidity, with concentrations reaching six times those found in the spring. With the exception of station 2, late summer turbidity exceeded early summer turbidity. Comparatively low turbidity levels were maintained from mid-July to mid-August, were decreased in September, and were increased in November. This pattern in turbidity followed erosion events with initial increases in turbidity after snowmelt and seedbed preparation. Summer increases followed rainfall events. In September, erosion potential was lower because crop coverage was at a maximum, rainfall events were less intensive, and no crop

maintenance was practiced. The increase in turbidity in November followed soil disturbance by crop harvesting. The spike in turbidity at station 1 is most likely attributed to extensive drain-reconstruction activities at this site during the sampling period. Station 6 turbidity levels were lower than 100 JTU due to the dilution effect of Lake Erie water.

Suspended Particulate Matter

Suspended particulate matter concentrations (Table 5) at station 6 were also low due to dilution by Lake Erie water. There is also no farmland adjacent to this station. The

Table 6 Concentrations (mg/L) of hardness (CaCO₃) in Muddy Creek

Sampling date	Station 1	Station 2	Station 3	Station 4	Station 5	Station 6
10 February	384	–	385	284	141	126
20 April	255	–	230	–	179	114
26 May	263	385	314	229	154	–
27 May	–	–	–	228	–	116
8 June	229	225	203	174	–	–
9 June	226	–	251	–	147	–
28 June	193	212	199	–	–	–
29 June	310	–	286	214	132	111
30 June	348	–	308	–	–	–
12 July	273	251	–	–	–	–
13 July	390	–	268	183	132	–
14 July	193	–	221	–	130	112
27 July	503	285	311	199	128	116
28 July	523	–	310	–	–	–
10 August	654	–	254	170	118	115
30 August	–	252	272	198	133	115
28 September	392	663	235	177	149	115
3 November	574	528	–	182	125	114

Table 7 Concentrations (mg/L) of alkalinity (CaCO₃) in Muddy Creek

Sampling date	Station 1	Station 2	Station 3	Station 4	Station 5	Station 6
10 February	185	–	228	174	111	93
20 April	156	–	150	–	131	94.6
26 May	208	226	212	168	112	–
27 May	–	–	–	167	–	89.1
8 June	86.5	87.8	83	75.6	–	86.1
9 June	114.5	–	117	–	78.4	–
28 June	75.5	94.5	96.1	–	–	–
29 June	155	–	159.5	124	94	82.4
30 June	189	–	179	–	–	–
12 July	158	158	–	–	–	–
13 July	242	–	181	133	106	–
14 July	97	–	135	–	104	87.7
27 July	260	–	271	179	108	92.8
28 July	267	233	276	–	–	–
10 August	280	284	264	152	93.9	87.5
30 August	–	224	310	186	108	91
28 September	209	138	160	161	130	90.3
3 November	245	208	–	208	146	101

concentrations of SPM were greater at station 4 in Muddy Creek compared with the other stations. These greater concentrations may be the result of bottom sediment resuspension caused by fish movements and wind-driven seiches. Sampling at this site also involved wading out into the creek to suspend the centrifuge pumps. This movement could also have caused resuspension of bottom sediment.

Attempts were made to limit this influence by placing the pumps upstream of the person handling the pumps.

In general, concentrations of SPM increased in late spring and late fall after soil disturbance caused by plowing and harvesting, respectively. The lack of an increase in SPM at station 4 may indicate the ability of riparian wetland to trap sediments. SPM increases in June and August

Fig. 7 Particulate P concentrations (mg/L) for the Muddy Creek watershed

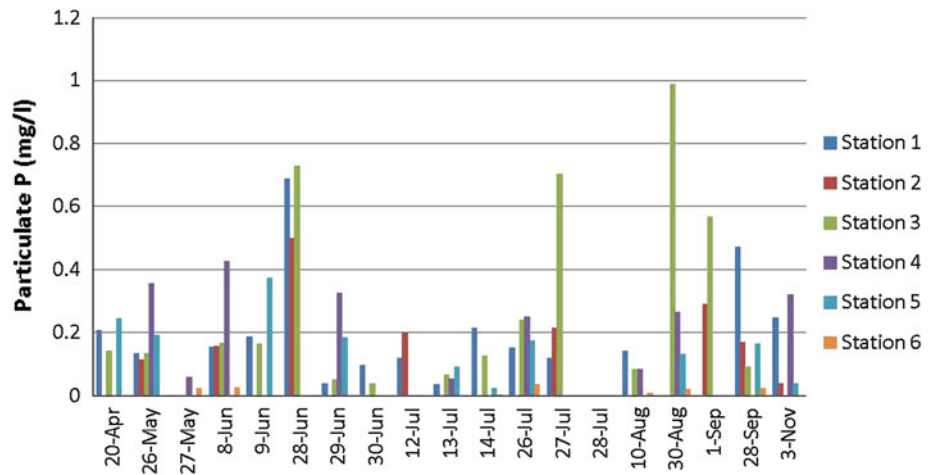
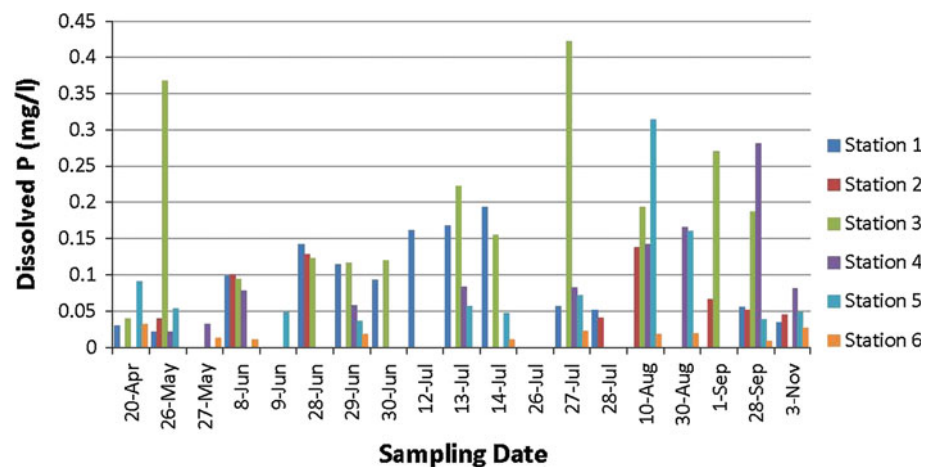


Fig. 8 Dissolved P concentrations (mg/L) for the Muddy Creek watershed



at stations 1 through 5 followed seasonally large rainfall events, 33 and 15 mm, respectively. Because stations 1 through 3 have much shallower water depth than the other stations and are bordered by field on either side of the creek, they may be more susceptible to land use and climatic influences and therefore greater increases in SPM, notably the 506 and 671 mg/L peaks in late June.

Water Hardness

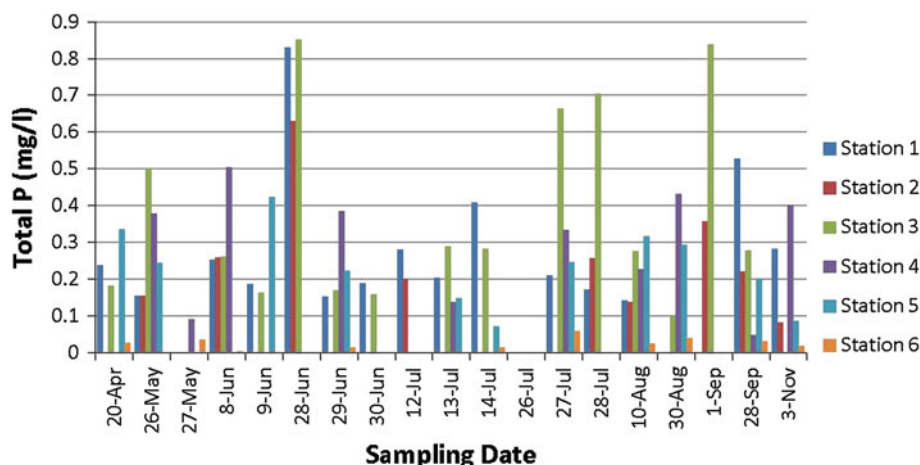
Water hardness can reflect biological activity with hardness increasing as productivity increases. The hardness of Muddy Creek water (Table 6), however, did not exhibit statistically significant relationships with DO or DOC. Hardness also reflects the geochemistry of underlying bedrock and soil. The Muddy Creek watershed is located on a till plain with underlying limestone, dolomite, and gypsum. Muddy Creek waters ranged from moderately hard (50–150 mg/L as CaCO₃) to very hard (>300 mg/L as CaCO₃) with hardness decreasing with progression downstream. Drinking-water standards for hardness (Canadian

Council of Ministers of the Environment 2011) were exceeded at stations 1 and 3.

Alkalinity

Waters with high alkalinity are undesirable for domestic uses primarily because of the associated hardness. Alkalinity levels (Table 7) in Muddy Creek fell within the acceptable range for drinking-water (30–500 mg/L as CaCO₃). The lowest alkalinity occurred in June at all stations. This decrease is associated with precipitation of CaCO₃ and the production of organic C and consumption of HCO₃⁻ by photosynthesizing phytoplankton (Schlesinger 1991). Maximum levels occurred in August at stations 1 through 3 and in November at stations 4 through 6. Increases in alkalinity follow from the consumption of CO₂ by bacterial decomposition. The increase in alkalinity at downstream stations in November may have been due to decomposition because it takes more time for phytoplankton to settle in deeper waters.

Fig. 9 TP concentrations (mg/L) for the Muddy Creek watershed



Particulate and Dissolved P

In general, particulate P concentrations exceeded dissolved P concentrations (Figs. 7, 8). On few occasions, dissolved P concentrations exceeded particulate P concentrations in late summer. In late summer, bacteria consume particulate P, with carbon (C) as a food source, during the degradation of organic matter. The bacteria then excrete P and C in their dissolved form. The concentrations of dissolved P during late summer in Muddy Creek varied from station to station. Sharpley and Menzel (1987) suggested that the leaching of nutrients from vegetation in different stages of growth and decomposition may partly account for seasonal fluctuations in dissolved P. Late summer dissolved P concentrations were greater than those in late May and early June (after fertilization of fields).

Increases in particulate P concentrations in June, July, and September were coincident with increases in primary productivity. A large portion of soluble P may be incorporated into algal tissues and organic debris rather than inorganically bound (Driscoll and others 1993).

Ratios of the percentage of dissolved P to the percentage of particulate P ranged from 0.005–16.732. At each of the stations, the percent that dissolved and particulate forms contributed to the TP concentration was similar in July and August and varied among stations. The ratios indicated that

the relative contribution of each type of sediment P to TP were comparable. The importance of particulate P relative to dissolved P was different for each site. The most similar ratios occurred in spring and fall corresponding to erosion events, such as plowing and harvesting activities.

Total Phosphorus

The concentration of TP is important, in general, as an indicator of a water body's eutrophication potential. TP (Fig. 9) concentrations in Muddy Creek exceeded critical concentrations (0.02 mg/L) with respect to surface water eutrophication (Sugiharto and others 1994). TP concentrations in Muddy Creek exceeded this criterion by at least one order of magnitude.

Environment Canada water-quality guidelines for TP concentrations range between 0.035 and 0.100 mg/L for the protection of freshwater aquatic life and 0.100 and 0.065 mg/L for drinking-water supplies (Canadian Council of Ministers of the Environment 2011). With the exception of station 6, concentrations of TP in Muddy Creek exceeded these guidelines. Concentrations of TP were greatest at station 3 and lowest at station 6. Concentrations of TP at these stations fluctuated throughout the sampling season, with the greatest concentrations occurring in the summer months (June through August).

Table 8 Distribution of major elements in surficial sediments in Muddy Creek (% dry weight)

Sampling station	SiO ₂	Al ₂ O ₃	Fe ₂ O ₃	MnO	MgO	CaO	K ₂ O	Na ₂ O	P ₂ O ₅
1	48.11	10.81	4.23	0.05	3.14	9.85	2.23	0.66	0.20
3	47.13	12.26	4.71	0.05	3.24	9.67	2.18	0.54	0.20
4	45.72	12.69	4.84	0.06	3.05	9.51	2.29	0.59	0.30
5	46.33	13.07	3.93	0.06	3.35	10.19	2.22	0.65	0.20
6	48.81	10.89	4.25	0.07	3.46	9.53	2.08	0.63	0.20

Detection limits: K₂O 0.05 %, P₂O₅ 0.03 %, and all others 0.01 %

Table 9 Concentration profiles of major elements in core sediments at station 4, Muddy Creek (% dry weight)

Depth (cm)	SiO ₂	TiO ₂	Al ₂ O ₃	Fe ₂ O ₃	MnO	MgO	CaO	Na ₂ O	K ₂ O	P ₂ O ₅
0–1	57.03	0.76	14.33	4.97	0.05	1.75	1.72	0.66	2.97	0.42
1–2	57.44	0.77	14.16	4.86	0.04	1.72	1.70	0.63	2.98	0.44
2–3	56.90	0.75	13.99	4.74	0.04	1.68	1.61	0.68	2.99	0.39
3–4	57.78	0.73	13.82	4.64	0.04	1.64	1.61	0.64	2.95	0.36
4–5	58.02	0.75	13.99	4.85	0.04	1.77	1.67	0.66	2.93	0.34
5–6	58.66	0.75	14.24	4.95	0.04	1.79	1.66	0.64	2.95	0.37
6–7	60.03	0.70	13.61	4.38	0.04	1.56	1.66	0.74	2.86	0.32
7–8	58.59	0.72	13.55	4.47	0.04	1.58	1.63	0.84	2.96	0.32
8–9	59.09	0.72	13.72	4.52	0.04	1.60	1.70	0.73	2.96	0.35
9–10	59.88	0.75	13.99	4.65	0.04	1.64	1.67	0.75	2.90	0.30
10–11	59.24	0.72	13.84	4.50	0.04	1.58	1.63	0.67	2.83	0.36
11–12	59.77	0.72	13.62	4.52	0.04	1.60	1.72	0.73	2.82	0.36
12–13	59.24	0.73	13.42	4.45	0.04	1.56	1.68	0.75	2.73	0.35
13–14	59.70	0.73	13.60	4.50	0.04	1.58	1.71	0.74	2.74	0.38
14–15	60.00	0.74	13.69	4.51	0.04	1.60	1.68	0.84	2.78	0.33
15–16	59.30	0.72	13.41	4.41	0.04	1.56	1.67	0.75	2.72	0.34
16–17	58.11	0.72	13.62	4.48	0.04	1.61	2.07	0.67	2.81	0.36
17–18	57.95	0.71	14.37	4.71	0.04	1.71	2.00	0.62	2.82	0.39
18–19	55.40	0.71	14.73	4.76	0.03	1.64	1.43	0.48	2.97	0.45
19–20	55.09	0.73	14.89	4.84	0.03	1.65	1.29	0.45	2.99	0.35
20–21	54.40	0.74	14.86	4.95	0.04	1.65	1.55	0.41	3.01	0.67
21–22	55.07	0.76	15.33	5.10	0.04	1.71	1.28	0.43	3.06	0.43
22–23	54.18	0.74	15.22	5.06	0.04	1.68	1.30	0.48	3.08	0.45
23–24	53.64	0.72	15.08	5.03	0.04	1.66	1.23	0.44	3.08	0.45
24–25	53.90	0.75	15.27	5.47	0.04	1.72	1.26	0.44	3.14	0.66

Detection limits: K₂O 0.05 %, P₂O₅ 0.03 %, and all others 0.01 %

Sediments

Surficial sediments were composed of primarily clay-sized particles. Surficial sediment composition ranged from 0 to 16.07 % gravel, 4.2–10.5 % sand, 16.8–32.8 % silt, and 57.5–72.7 % clay. Particle-size distribution of SPM could not be quantitatively determined due to distortion of particles during centrifuging.

The concentrations of major elements in surficial sediments were similar among the sampling stations (Table 8) and indicated a similar geochemical composition within Muddy Creek (Bourgoin and others 1994). Silica, Al₂O₃, and CaO represented the largest part of the sediments' geochemical composition. High concentrations of Ca were expected because Muddy Creek drains a watershed underlain by limestone. The concentration of Al, a constituent of clay minerals (Mudroch and Duncan 1986), reflected the predominant soil type in the watershed, i.e., Brookston clays. The concentrations of P in surficial sediments were similar at stations 1, 3, 5, and 6 with slightly greater concentrations at station 4. The concentrations of P

in SPM were up to three times greater than those in surficial sediments. Mudroch (1984), with similar results in several southern Ontario marshes, found that the greater concentration of P in SPM indicated regeneration of P within the water column. The predominance of fine-grained-sized particles also indicated the settling out of SPM during low-flow conditions; this can serve as a potential source of P through desorption from surficial sediments in the streambed during anoxic conditions (Driscoll and others 1993) or when algal consumption reduces the dissolved P concentration in the water lower than that of the equilibrium P concentration between particulate and dissolved P (Oloya and Logan 1980).

The geochemical composition of the sediment core collected at station 4 (Table 9) indicated past inputs of geochemically similar material (Bourgoin and others 1994). ²¹⁰Pb dating indicated that either little sediment accumulation had occurred at this site in the last 150 years or that this site is an area with cyclic deposition and removal of fine-grained sediments with subsequent transport downstream (Turner 1994). Bourgoin and others

Table 10 Summary of seasonal AGNPS output data at the Muddy Creek watershed outlet for rainfall events: spring (May 15), summer (July 8), and fall (November 1)

AGNPS output	Spring	Summer	Fall
A. Existing conditions			
Runoff volume (mm)	7.6	25.4	2.5
Peak runoff rate (m ³ /s)	2.7	9.5	1.0
TPS (kg/ha)	0.01	0.03	0.01
Total soluble P in runoff (kg/ha)	0.25	0.61	0.09
Soluble P in runoff (mg/L)	3.85	2.43	4.29
B. Summer fallow conditions			
Runoff volume (mm)		33.0	
Peak runoff rate (m ³ /s)		12.5	
TPS (kg/ha)		0.03	
Total soluble P in runoff (kg/ha)		1.25	
Soluble P in runoff (mg/L)		3.78	
C. Winter wheat cover crop alternative–management option			
Runoff volume (mm)	5.1	20.3	2.5
Peak runoff rate (m ³ /s)	2.1	8.3	0.7
TPS (kg/ha)	0.01	0.02	0.01
Total soluble P in runoff (kg/ha)	0.11	0.30	0.03
Soluble P in runoff (mg/L)	2.4	1.45	2.19
D. No-till/corn residue alternative–management option			
Runoff volume (mm)	7.6	25.4	2.5
Peak runoff rate (m ³ /s)	2.7	9.5	0.96
TPS (kg/ha)	0.01	0.03	0.01
Total soluble P in runoff (kg/ha)	0.17	0.42	0.06
Soluble P in runoff (mg/L)	2.61	1.66	2.85

(1994) found that pesticide concentrations in the sediment at this station supported the second scenario. Station 4 is located at the point in the creek where wind-induced seiches travelling upstream meet the downstream flow.

NPS-Pollution Potential

Agricultural non-point source pollution model results for Muddy Creek showed runoff volumes, peak runoff rates, and total soluble P (an indication of fertilizer loss) concentrations

in runoff comparable with those in spring and summer and marked decreases in the fall (Table 10). In general, summer erosion losses and sediment yields exceeded spring and fall losses and yields, respectively (Tables 11, 12, 13, 14, 15 and 16). The greatest concentrations of the aforementioned parameters occurred under existing summer and fallow conditions (Tables 11, 12, 13, 14, 15 and 16). The use of a winter wheat cover crop as an alternative to leaving a field fallow was most effective in decreasing soil erosion losses (25–30 %) in summer and fall. Using a no-till/corn residue combination was most effective at decreasing soil erosion loss during the spring (20–30 %).

Rainfall intensity and amount were the primary influences on runoff volume and peak runoff rate, with summer storm events having the greatest erosive potential and subsequently the highest predicted total P concentrations (Table 10). Runoff volume, in turn, was the primary influence on erosional losses. Secondary influences on erosion were soil erodibility (*K*-factor) and slope gradients. Total P in sediment (TPS) and dissolved P followed seasonal trends similar to erosional loss and sediment yield. In addition to runoff volume and soil erosion, fertilizer P availability in the Muddy Creek watershed (Fig. 10) was a function of the method of fertilizer application. Most fertilizers were broadcast at the time of application with no incorporation, leaving fertilizers available for erosion and runoff.

The greatest predicted losses of soils and available P were from the upper reaches of the watershed associated with soil *K*-factors of 0.13–0.16 (Fig. 11). These losses also reflect land use and management practices in the adjacent fields, i.e., continuous row cropping, spring seedbed cultivation, and fall moldboard plowing, which all expose soil to erosion.

Because the purpose of running the AGNPS model for the Muddy Creek watershed was to perform an initial screening of potential source areas, the limited observed data were used for model validation and not model calibration and sensitivity analysis. AGNPS was designed to respond to standard input values selected according to observed watershed conditions and can be run without calibration (Enright and Madromootoo 1990; Overcash and

Table 11 AGNPS output data at location 1, Muddy Creek watershed

AGNPS output	Spring			Summer				Fall		
	Existing conditions	Winter wheat	No-till/corn residue	Existing conditions	Worst case	Winter wheat	No-till/corn residue	Existing conditions	Winter wheat	No-till/corn residue
Runoff volume (mm)	5.6	3.8	5.6	23.9	34.0	19.8	23.9	1.5	0.8	1.5
Peak runoff rate (m ³ /s)	0.74	0.51	0.74	2.72	3.71	2.32	2.72	0.20	0.11	0.20
Sediment yield (t/ha)	3.77	1.73	2.85	16.81	10.45	3.21	7.96	1.52	0.45	1.57
TPS (kg/ha)	0.02	0.01	0.02	0.09	0.06	0.02	0.04	0.01	0	0.01
Dissolved P (kg/ha)	0.62	0.27	0.44	1.51	3.06	0.74	1.06	0.22	0.07	0.15

Table 12 AGNPS output data at location 2, Muddy Creek watershed

AGNPS output	Spring			Summer				Fall		
	Existing conditions	Winter wheat	No-till/corn residue	Existing conditions	Worst case	Winter wheat	No-till/residue	Existing conditions	Winter wheat	No-till/corn residue
Runoff volume (mm)	5.6	3.8	5.6	23.9	34.0	19.8	23.9	1.5	0.8	1.5
Peak runoff rate (m ³ /s)	1.53	1.08	1.53	5.81	7.99	4.93	5.81	0.42	0.23	0.42
Sediment yield (t/ha)	7.91	4.15	5.92	41.3	28.72	6.28	17.93	3.68	0.94	3.70
TPS (kg/ha)	0.03	0.02	0.02	0.12	0.09	0.03	0.07	0.02	0.01	0.02
Dissolved P (kg/ha)	0.64	0.30	0.40	1.53	3.16	0.74	0.96	0.22	0.07	0.15

Table 13 AGNPS output data at location 3, Muddy Creek watershed

AGNPS output	Spring			Summer				Fall		
	Existing conditions	Winter wheat	No-till/corn residue	Existing conditions	Worst case	Winter wheat	No-till/residue	Existing conditions	Winter wheat	No-till/corn residue
Runoff volume (mm)	5.6	3.8	5.6	23.9	34.0	19.8	23.9	1.5	0.8	1.5
Peak runoff rate (m ³ /s)	1.84	1.33	1.84	7.11	9.74	6.00	7.11	0.54	0.28	0.54
Sediment yield (t/ha)	12.26	5.83	9.03	67.58	48.24	9.01	28.87	5.36	1.26	5.49
TPS (kg/ha)	0.03	0.02	0.02	0.13	0.10	0.02	0.07	0.02	0	0.02
Dissolved P (kg/ha)	0.59	0.30	0.42	1.41	3.16	0.77	1.01	0.22	0.07	0.15

Table 14 AGNPS output data at location 4, Muddy Creek watershed

AGNPS output	Spring			Summer				Fall		
	Existing conditions	Winter wheat	No-till/corn residue	Existing conditions	Worst case	Winter wheat	No-till/residue	Existing conditions	Winter wheat	No-till/corn residue
Runoff volume (mm)	5.6	3.8	5.6	23.9	34.0	19.8	23.9	1.5	0.8	1.5
Peak runoff rate (m ³ /s)	1.84	1.30	1.84	7.16	9.74	6.06	7.16	0.54	0.28	0.54
Sediment yield (t/ha)	8.52	4.19	6.41	45.59	29.48	6.93	20.53	3.77	0.96	3.83
TPS (kg/ha)	0.02	0.01	0.01	0.07	0.06	0.01	0.03	0.01	0	0.01
Dissolved P (kg/ha)	0.64	0.27	0.40	1.56	2.99	0.74	0.96	0.25	0.07	0.15

Davidson 1989). Model performance was evaluated by the statistical comparison of observed and predicted (modeled) data.

We employed the Nash–Sutcliffe coefficient to measure the goodness of fit between model predictions and measured data (Nash and Sutcliffe 1970):

Table 15 AGNPS output data at location 5, Muddy Creek watershed

AGNPS output	Spring			Summer				Fall		
	Existing conditions	Winter wheat	No-till/corn residue	Existing conditions	Worst case	Winter wheat	No-till/corn residue	Existing conditions	Winter wheat	No-till/corn residue
Runoff volume (mm)	5.6	3.8	5.6	23.9	34.0	19.8	23.9	1.5	0.8	1.5
Peak runoff rate (m ³ /s)	2.32	1.73	2.32	8.81	11.72	7.56	8.81	0.74	0.45	0.74
Sediment yield (t/ha)	8.94	2.42	4.82	33.69	27.33	3.97	18.22	2.76	0.67	3.27
TPS (kg/ha)	0.01	0	0.01	0.04	0.03	0.01	0.02	0.01	0	0.01
Dissolved P (kg/ha)	0.57	0.27	0.37	1.36	2.82	0.69	0.91	0.20	0.07	0.12

Table 16 AGNPS output data at location 6, Muddy Creek watershed

AGNPS output	Spring			Summer				Fall		
	Existing conditions	Winter wheat	No-till/corn residue	Existing conditions	Worst case	Winter wheat	No-till/corn residue	Existing conditions	Winter wheat	No-till/corn residue
Runoff volume (mm)	7.6	5.1	7.6	25.4	33.0	5.1	25.4	2.5	1.5	2.5
Peak runoff rate (m ³ /s)	2.69	2.10	2.69	9.54	12.55	8.30	9.54	0.96	0.68	0.96
Sediment yield (t/ha)	6.41	6.59	8.85	28.56	22.17	14.39	22.48	2.78	3.18	5.18
TPS (kg/ha)	0.01	0	0.01	0.03	0.03	0.02	0.03	0.01	0.01	0.01
Dissolved P (kg/ha)	0.54	0.25	0.37	1.33	2.74	0.67	0.91	0.20	0.07	0.12

$$E = 1 - \left[\frac{\sum_{i=1}^N (O_i - M_i)^2}{\sum_{i=1}^N (O_i - \bar{O})^2} \right],$$

where O_i is the observed values at station i , M_i is the modeled value at site i , \bar{O} is the average of the observed values at all sites, and N is the total number of sites. E can range from $-\infty$ to 1. Values between 0.0 and 1.0 are considered acceptable, with goodness of fit increasing toward a perfect match of 1. Values <0.0 indicate that the observed value is a better estimate than the predicted value. In addition, we used the percent bias to measure the average tendency of the modeled data to be larger or smaller than observed data (Meixler and Bain 2010):

$$\text{Percent bias} = \left[\frac{(\sum_{i=1}^N (O_i - M_i) \times 100)}{(\sum_{i=1}^N (O_i))} \right].$$

The optimal percent bias value is one, with positive values indicating model underestimation bias and negative values indicating model overestimation bias.

We compared observed dissolved and particulate P concentrations with the AGNPS model output. The coefficients for our modeling period (April through November 1993) were

0.35 and 0.08, respectively. According to the model efficiency classification of Parajuli and others (2009), the model simulation for dissolved P is considered fair (0.25–0.49) and poor for particulate P (0.00–0.24). According to the percent bias of +57 and –36 % for particulate and dissolved P concentrations, the values fall within the acceptable but not accurate range for model simulation (Meixler and Bain 2010). The positive percent bias for particulate P indicated an underestimation bias, whereas the negative percent bias for dissolved P indicated an overestimation bias. The range of predicted P concentrations was comparable with those of observed ranges. Seasonal trends as predicted by AGNPS did correspond to the measured data for the watershed.

There is a scarcity of studies regarding validation of the AGNPS model using measured P data. LimnoTech (2010) found an underprediction of TP load during late to early spring and an overprediction during the summer and early fall. Huang and Hong (2010) found an overprediction of annual fluxes of TP. These two studies, however, did not distinguish between particulate and dissolved contributions to P load. Ng and others (1994) found AGNPS to

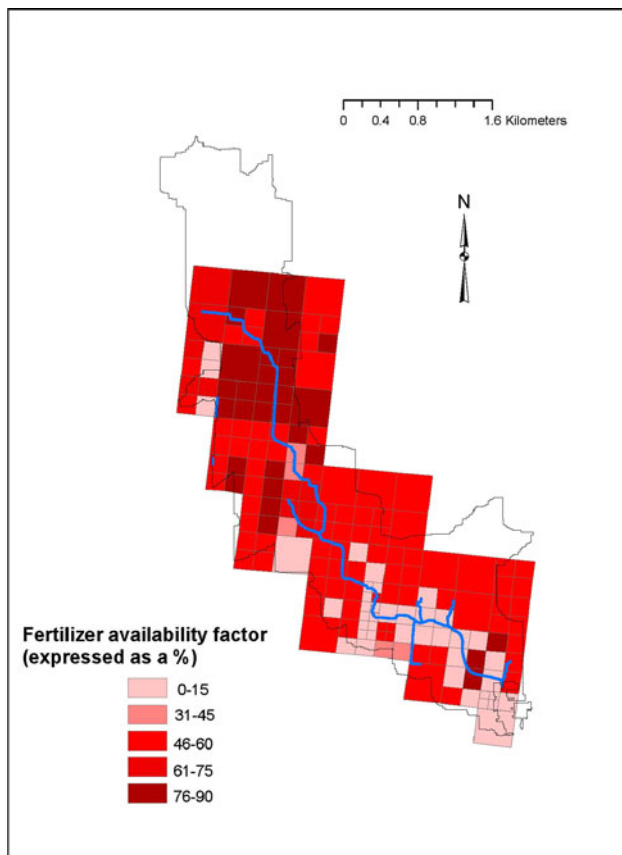


Fig. 10 Fertilizer-availability factor for the Muddy Creek watershed (AGNPS model output)

overpredict particulate P and dissolved P by a factor of 2.6 and 24, respectively. We found that particulate P was underestimated on average by a factor of 2.9 and dissolved P on average by a factor of 50.4. The model may not accurately represent in-stream losses and transformations of P (McFarland and Hauchk 2001). The P-cycling algorithms within AGNPS warrant further study.

The inaccuracy in P prediction may have also been a function of the observed data used for comparison. We used instantaneous point data at six locations to compare with 24-h event-based model output data. We expect the goodness of fit for the model to increase with storm event data, collected at several more locations, beyond one sampling season (Liu and others 2008). In addition to further validation analyses, parameter-sensitivity analysis is needed to investigate the sensitivity of P concentrations to spatially controlled physical properties, such as soil texture and erodibility, as well as temporal processes, such as land-cover change, including crop type coverage.

Although the AGNPS model did not accurately predict P loadings in the Muddy Creek watershed, it did predict seasonal trends and identified areas where BMPs would be most effective. The model also identified the winter wheat

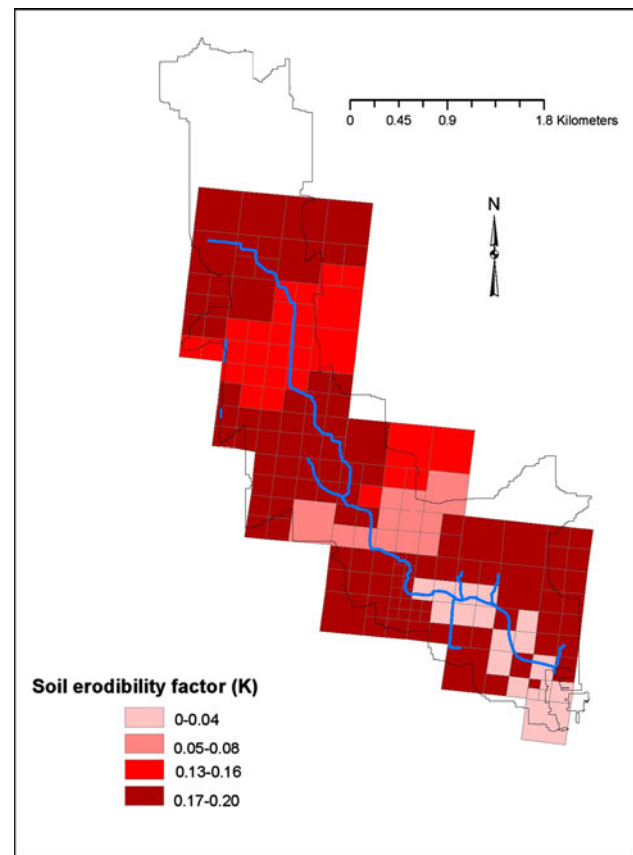


Fig. 11 K-factor for the Muddy Creek watershed (AGNPS model output)

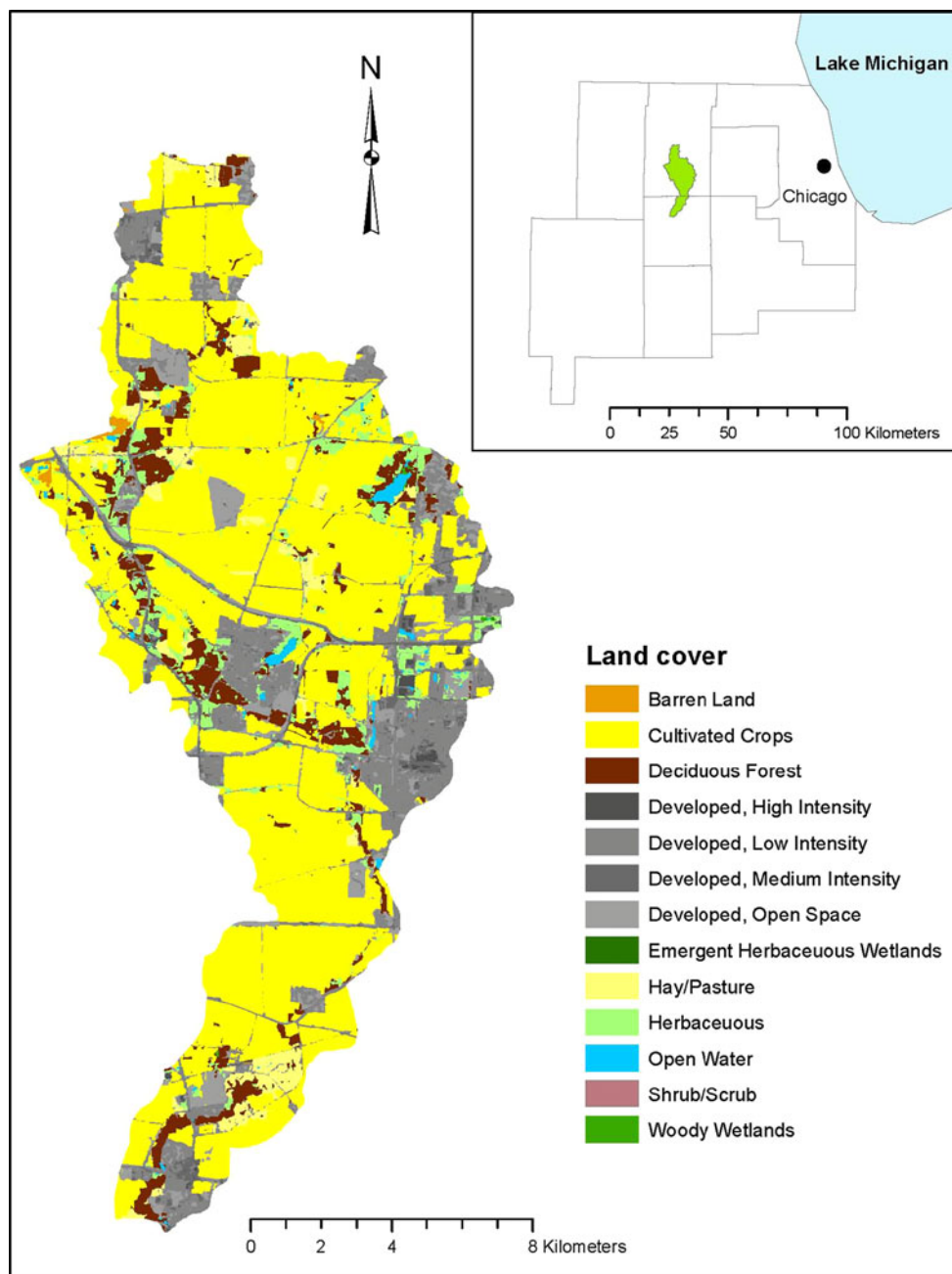
cropping–management system as the most effective management option in decreasing runoff volumes and erosion losses. The decreases were an improvement on observed cropping practices. The results showed that management practices that decrease sediment delivery to a surface water body, such as Muddy Creek, are effective in decreasing sediment-associated P loadings to these receiving water bodies.

Blackberry Creek Watershed

Study Area

The Blackberry Creek watershed drains a largely agricultural area of 189 km² located in northeastern Illinois, just west of the metropolitan area of Chicago (Fig. 12). The creek is a south-flowing tributary of the Fox River watershed and the greater Illinois–Mississippi River system spanning both Kane and Kendall Counties. Eleven percent of the state’s population (Illinois Department of Natural Resources 2009) lives within the Fox River watershed. The Fox River and its tributaries provide flood conveyance and

Fig. 12 Blackberry Creek watershed land-cover. (*Inset*) location of the watershed relative to Chicago, Illinois



drinking-water supplies to this population (Illinois Department of Natural Resources 2009). Among the top resource concerns in the Blackberry Creek watershed are flooding, soil erosion, and sediment control (Natural Resources Conservation Service 2010).

The average daily temperature is 8.8 °C, with July being the warmest month (daily mean 22.8 °C) and January the coldest month (daily minimum −3.3 °C). The length of the growing season is 165–170 days, with an average frost-free period of 160 days (Illinois State Water Survey 2009). Mean annual rainfall is 949.5 mm, with 45 % occurring June through September. Slopes are generally <2 %, and

soils in the watershed are primarily loams, silt loams, and silty clay loams of moderately slow to slow permeability.

The Blackberry Creek watershed is developing rapidly, with both population and proportion of urbanized land area in the watershed expected to double in the next 20 years. According to United States Census Bureau population estimates (United States Census Bureau 2010), the population in Kane County (currently 515, 269) increased 26.7 % from 2000 to 2009, placing it among the fastest growing counties in the state of Illinois. Cropland covers 56 % of the watershed with significant areas of natural grassland (28 %) and wetlands (3.7 %). Urban land use

currently represents 5.7 % of land use in the watershed (Fig. 12).

Research Approach

The Blackberry Creek watershed’s landscape is still primarily agricultural, but urban land continues to advance into the watershed, thus decreasing cropland coverage, which makes our watershed-modeling efforts less accurate because land-cover is one of the most important model parameters. Substantial changes in land-cover that urban fringe watersheds, such as Blackberry Creek are experiencing can significantly affect runoff, soil loss potential, and ultimately P loading to surface waters.

Therefore, the first step in building our watershed model is the development of a comprehensive spatial and temporal land-cover change component. ArcGIS (ArcInfo 10.0 ESRI Redlands, California) ModelBuilder was used to capture land-cover change in the watershed from 2001 to 2010 and to provide an annual update for 2008–2009. We developed a procedure (described later in the text) for determining the amount of agricultural land that is lost to urban development in a 1-year period so we can quickly feed that information into our model and determine the effects on model output.

Land-Cover Change

We used two satellite image-derived land-cover data sets for this analysis. The first was the 2001 National Land Cover Data set (NLCD). The second was the NASS cropland data layer (CDL), which was derived from satellite imagery obtained by the USDA–National Agricultural Statistics Service (NASS) on an annual basis. We decided to use NLCD (2001) and CDL (2010) because they both have national coverage for those years, and therefore this can be replicated for any location in the United States. The USDA processed the raw satellite imagery by classifying the imagery into land-cover categories as listed in Table 17. The land-cover classification systems for NLCD 2001 and NASS 2010 are standardized to NLCD categories. To illustrate our procedure, we chose to work with the 2001 NLCD as the beginning period and the latest available 2010 CDL for the end of the change period. Before 2009, only selected states had CDL data available, but now the coverage is national in scope, which makes our procedure all the more relevant because it can be replicated across the United States.

The CDL data are in a raster format, so we begin our land-cover change model in the Spatial Analyst, an ArcGIS extension used for raster data. In the first process, we select out the urban land-cover categories for both 2001 and 2010 (Fig. 13). We call these our “Extract 2001 Urban” and “Extract 2010 Urban” tools, which are coded with the

Table 17 Land-cover classification codes for NASS cropland data layer

Code	Land-cover
1	Corn
4	Sorghum
5	Soybeans
21	Barley
23	Spring wheat
24	Winter wheat
26	Winter wheat/soybeans double-cropped
27	Rye
28	Oats
36	Alfalfa
42	Dry beans
43	Potatoes
44	Other crops
47	Miscellaneous fruit and vegetables
53	Peas
58	Clover/wildflowers
61	Fallow/idle cropland
62	Grass/pasture/nonagricultural
63	Woodland
87	Wetlands
92	Aquaculture
111	NLCD-open water
121	NLCD-developed/open space
122	NLCD-developed/low intensity
123	NLCD-developed/medium intensity
124	NLCD-developed/high intensity
131	NLCD-barren
141	NLCD-deciduous forest
142	NLCD-evergreen forest
152	NLCD-shrubland
171	NLCD-grassland herbaceous
181	NLCD-pasture/hay
190	NLCD-woody wetlands
195	NLCD-herbaceous wetland

following Spatial Analyst “Single Output Map Algebra” statements:

$$(2001) \text{ con} ([\text{NLCD } 2001] = 121 \text{ or } [\text{NLCD } 2001] = 122 \text{ or } [\text{NLCD } 2001] = 123 \text{ or } [\text{NLCD } 2001] = 124, 1, 0)$$

$$(2010) \text{ con} ([\text{CDL } 2010] = 121 \text{ or } [\text{CDL } 2010] = 122 \text{ or } [\text{CDL } 2010] = 123 \text{ or } [\text{CDL } 2010] = 124, 1, 0).$$

The operation “con” is a conditional statement, and here it is stating that if the input land-cover raster layer’s value

Fig. 13 Flow diagram illustrating ArcInfo ModelBuilder process for selecting out urban land-cover categories from 2001 to 2010 cropland data layers

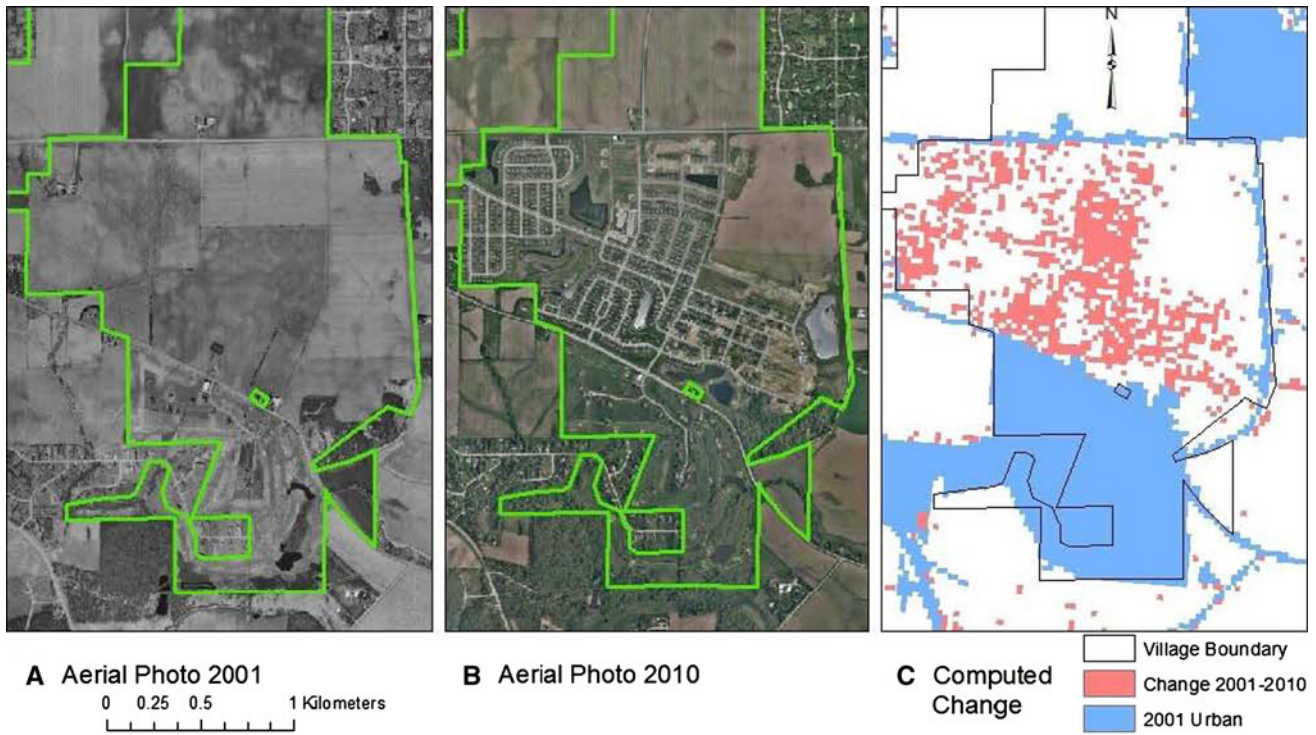
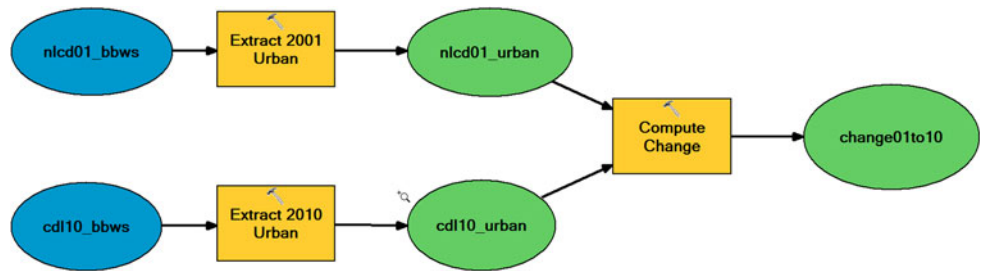


Fig. 14 High-resolution digital area photography (a and b) used to assess the accuracy of the land-cover change model (c)

equals one of four urban categories, then output to a new raster where pixel values will be one for urban and assign zero for all other pixels. In the second process, we use the following Spatial Analyst “Map Algebra” statement to select out the new urban land that has appeared between 2001 and 2010 and call it our “Compute Change” tool:

$$\text{con}([\text{Urban 2001}] < > 1 \text{ and } [\text{Urban 2010}] == 1, 1, 0).$$

This conditional operation is stating that if the first input, the 2001 urban raster, is not equal to urban (value of one) and the second input, the 2010 urban raster, is equal to urban (value of one), then output to a new raster where pixel values will be one for nonurban to urban conversions for the 2001–2010 period and assign zero for all other pixels.

Once we ran our land-cover change model, we needed to evaluate its accuracy. High-resolution digital aerial

photography was available for both 2001 and 2010 for the entire watershed, which allowed us to ground-truth the urban change (Fig. 14). Figure 14a shows an area in the northern part of the watershed, near the village of Elburn, where in 2001 the urban land is intermixed with agricultural land. Using aerial photo-interpretation techniques, one can see in the inset for Fig. 14a that the land is all agricultural, whereas the inset for Fig. 14b shows that by 2010 the area had been converted into urban land. Figure 14c shows the urban land in 2001 in blue, whereas the change picked up in our model is shown in red. Our annual change analysis (2008–2009) shows how our procedures can capture more subtle urban change during a development down cycle. We introduce this annual analysis to demonstrate how we could capture annual change with these techniques. Although there was nationwide coverage of CDL in 2009, we decided not to compare CDL 2009

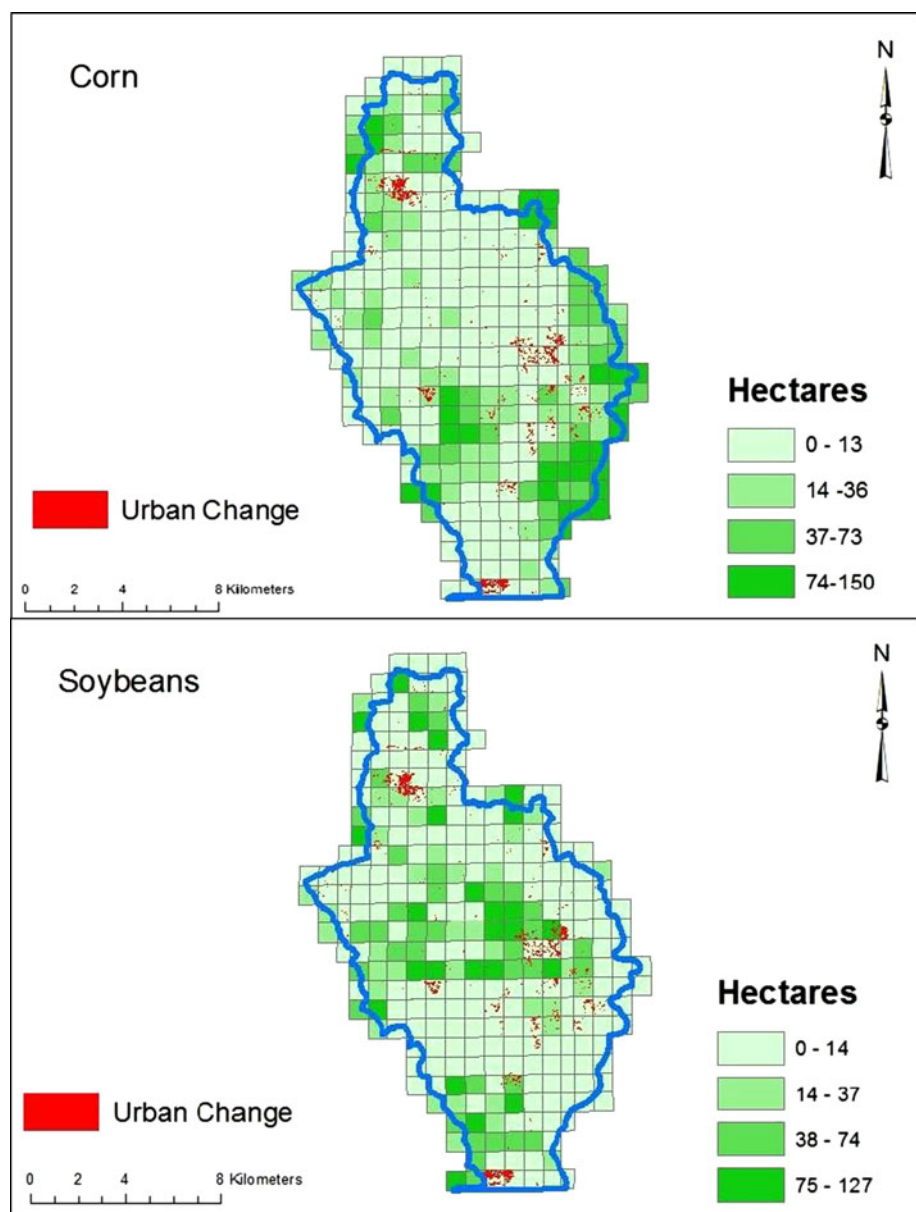
with CDL 2010 because they had different cell resolutions, that is, the 2009 CDL has a 56-m cell size, whereas the 2010 CDL has a 30-m resolution. A test of the latter showed significant misalignments resulting from these cell size differences. Misalignments were also noted in a land-cover change analysis by Thompson and Prokopy (2009), who provide correction methodologies. The 2008–2009 analysis used consistent pixel sizes (56 m each), but the change we detected was minimal because the period was moving downward in the development cycle. Changes detected were of an infill nature, e.g., land that was in development transition in 2008 was completed in 2009.

Once the urban change model steps are completed, the results can be incorporated into our watershed model layer. A grid polygon (shapefile) was used to capture the spatial

data (DEMs, hydrology, soils, and crop type). Raster data were converted to polygons, and a spatial intersection was performed. This process created a “fishnet” (a grid with cells represented as polygons) containing different parameters stored in different fields. Corn and soybean coverage are key parameters (because they have the most potential for soil erosion and P availability), so we are able to adjust our coverages of these crops by subtracting the urban change hectares from these cropland totals and rerunning the model (Fig. 15).

Our watershed-model map layer is composed of one-quarter quarter-section polygons (parcels [16.2 ha]), which form the basis of farm property boundaries in the Blackberry Creek watershed. Many states use parcels to identify land ownership. Parcels are identified by geographic

Fig. 15 Changes to crop coverage in hectares for corn (*top panel*) and soybeans (*bottom panel*)



coordinates and the township and range sections of the Public Land Survey System (PLSS). Choosing a grid cell size coincident with a PLSS section allows for applicability of the model to areas other than the pilot watersheds. These data are readily available because many counties maintain parcel geo-databases. In addition, farm management units comprise individual/multiple contiguous/noncontiguous parcels that are easily analyzed using the spatially distributed approach of the grid.

Management Implications

Water quality is affected by a combination of natural and anthropogenic factors, the relative influences of which change with spatial and temporal scale. Management decisions are thus complex and require a distributed modeling approach. Distributed models, in which input parameters are specified for individual grid cells, are considered more spatially accurate in the prediction of NPS pollution (Leon and others 2002).

Although the linking of distributed-parameter models, such as AGNPS to GIS, facilitates data input and manipulation and produces a detailed spatially displayed output (Liao and Tim 1997), the models are time and training intensive. The task of building extensive parameter input files and the high requirements for analysis of model results and computation efficiency due to the complexity of such models has hindered the effective application and use of these models by resource managers (Singh and others 2005).

Geographic information systems provide effective tools to generate, manipulate, and organize the spatially disparate data needed for modeling NPS pollution (Wu and others 2005) using readily available spatial data sets with easily understood graphic outputs. Our GIS protocol represents individual grid cells as unique polygons based on quarter-section parcels of land. We integrated various data sets to this unique set of polygons to allow for the future evaluation of various BMP scenarios through database manipulation. The model output is one set of unique polygons with numerous related data sets; this allows for the simultaneous modeling of spatial and temporal variability in multiple landscape attributes. Due to the grid cell nature of the model, other variables, such as runoff, can be aggregated to the same quarter-sections or scaled up or down as needed. The AGNPS model was developed primarily for use in agricultural watersheds. In this study, sediment and P loadings under baseline crop-stage conditions and several BMP strategies were simulated. We contribute to the literature on AGNPS validation for P and despite simulation shortcomings in this regard, we showed that the model is still a valuable tool in identifying critical sources areas of NPS pollution and in analyzing the change

in NPS pollution potential as a consequence of alternative BMPs.

Land-cover change in AGNPS is handled through iterative runs of the model, such as the BMP scenarios investigated in our study. Land-cover change is accounted for by changing the model input parameters accordingly. One of the benefits of the land-cover change model we developed for the Blackberry Creek watershed is the ability to link this protocol to our fishnet grid analysis, thus facilitating the use of satellite imagery to assess land-cover change by linking it to key parameters (in our case, corn and soybean crop changes) rather than having to change multiple input parameters.

By developing a method to assess urban land-cover change, we have expanded the applicability of our model to mixed-use watersheds (Hamlett and others 1992). Our results are relevant to local and regional planners interested in investigating both short- and long-term responses of water resources to land use change and BMPs (Praskievicz and Chang 2011). Land use type is one of the most important factors that affect uncertainty in NPS pollution simulation; this is critical to the overall simulation procedure because land use is a critical factor impacting the variance of NPS (Shen and others 2010). Urban land advancement is particularly important to parameterize accurately because it affects both spatial and temporal variance in NPS-pollution potential (Manonmani 2010).

We have provided a tool that can be used at different levels of planning from individual farm management to the watershed scale by key stakeholders, such as local government information management offices and county planners, as a decision support tool for targeting conservation and mitigation efforts (Huang and Hong 2010). The primary advantages of our model are minimal data preprocessing, accessibility of data, useful graphic output and output scale, and widespread applicability (Wu and others 2005). Meixler and Bain (2010) provide a comprehensive list of the potential advantages of GIS NPS models, including their usefulness in regions with limited current water-quality information, their ability to be executed by organizations with in-house GIS capabilities, and their generalizability at the regional scale.

As with other simplified GIS NPS models, we provide the caveat that our model is not meant for watersheds where actual concentration level data predictions are needed or where BMPs will be based solely on model output (Meixler and Bain 2010). Rather, we propose a methodology that may be useful for resource managers in initial watershed screening and the identification of PSAs where more in-depth study should occur (Hamlett and others 1992). PSAs of pollution often contribute the greatest pollution load to a watershed and significantly affect receiving water quality (Srinivasan and McDowell 2009). Control measures decrease NPS pollution to a greater

extent and are most cost-effective if they are implemented on targeted PSAs (McDowell and others 2001; Hamlett and others 1992).

Conclusion

We have showed the useful and practical application of GIS methods for the determination of the relative importance of land use change on stream water quality and NPS pollution potential in agricultural and urbanizing watersheds. We developed a protocol based on grid cell polygons. By aggregating watershed data to one standard grid cell size, based on land parcel ownership, we were able to develop GIS layers for the hydrophysical resources of the Muddy Creek watershed from disparate sources and scales. In addition, use of these polygons provides increased model functionality in terms of applicability to other watersheds and for investigations at varying scale in that numerous parameter values can be aggregated to the grid. We used this functionality to predict the relative potential sources of sediment and P-pollution in the Muddy Creek watershed as well as for postsimulation, georeferenced graphical display. Although the AGNPS model did not accurately predict P concentrations, it did provide a relative comparison of pollution potential severity in the watershed and provides a reasonable preliminary analysis for additional in-depth studies.

We also established new spatial techniques for the analysis of agricultural watersheds affected by land conversion to urban uses. Urban fringe watersheds provide a means of investigating both agricultural and rural/suburban residential activities as well as their relationship to each other and to NPS-pollution generation. We used ArcGIS ModelBuilder and Map Algebra to estimate change in short- and long-term land-cover changes in the Blackberry Creek watershed to better account for land use change, including changes to corn and soybean crop coverage where we expect more intensive farming practices and fertilization levels to affect NPS pollution potential. Future research will include building on this land-cover change component as a vehicle for modeling the implementation of BMPs, associated change in land use, and the effect on runoff quality at a variety of spatial and temporal scales. Further model sensitivity analysis will be used to refine model output for the purpose of site-specific targeting of NPS pollution where BMPs should be focused for optimal results; this will aid in soil and water conservation planning and contribute to more informed decision-making.

Acknowledgments Funding for this research was provided in part by Penn State Altoona, the National Sciences and Engineering Research Council of Canada, Agriculture and Agri-Food Canada (Centre for Land and Biological Resources Research), and Environment Canada (Canada Centre for Inland Waters). We thank Timothy

Dolney and Susan Enyedy-Goldner for their assistance with data acquisition, processing and editorial comments. We also acknowledge the intellectual contributions of S. Brian McCann and Bernard Bourgoin.

References

- Barco J, Hogue T, Curto V, Rademacher L (2008) Linking hydrology and stream geochemistry in urban fringe watersheds. *Journal of Hydrology* 360:31–47
- Bourgoin BP, Mudroch A, Garbai G (1994) Distribution of pesticides in streams and wetlands on the north shore of Lake Erie. National Water Research Institute, Burlington
- Canadian Council of Ministers of the Environment (2011) Canadian environmental quality guidelines. <http://ceqg-reqe.ccme.ca>. Accessed 12 Oct 2011
- David MB, Gentry LE (2000) Anthropogenic inputs of nitrogen and phosphorus and riverine export for Illinois, USA. *Journal of Environmental Quality* 29:494–508
- Driscoll CT, Effler SW, Auer MT, Doers SM, Penn MR (1993) Supply of phosphorus to the water column of a productive hardwater lake: controlling mechanisms and management considerations. *Hydrobiologia* 253:61–72
- Duncan GA, LaHaie GG (1979) Size analysis procedures. Sedimentology Laboratory, National Water Research Institute, Burlington
- Enright P, Madromootoo CA (1990) Application of the CREAMS hydrology component for runoff prediction in Quebec. ASAE paper number 90-2514. American Association of Agricultural Engineers, St. Joseph
- Environment Canada (2010a) Wheatley Harbour delisted areas of concern. <http://www.ec.gc.ca/raps-pas/Default.asp?lang=En&n=299C927C-1>. Accessed 1 Oct 2010
- Environment Canada (2010b) Canadian Climate Normals 1971–2000 for Point Pelee, Ontario. http://climate.weatheroffice.gc.ca/climate_normals/results_e.html?stnID=4606&lang=e&dCode=0&StationName=POIN&SearchType=Contains&province=ALL&provBut=&month1=0&month2=12. Accessed 15 Oct 2010
- Ghadouani A, Coggins LX (2011) Science, technology and policy for water pollution control at the watershed scale: current issues and future challenges. *Physics and Chemistry of the Earth* 36: 335–341
- Hamlett JM, Miller DA, Day RL, Peterson GW, Baumer GM, Russo U (1992) Statewide GIS-based ranking of watersheds for agricultural pollution prevention. *Journal of Soil and Water Conservation* 47:399–404
- Hoagland P, Anderson DM, Kaoru Y, White AW (2002) The economic effects of harmful algal blooms in the United States: estimates, assessment issues and information needs. *Estuaries* 25:819–837
- Huang J, Hong H (2010) Comparative study of two models to simulate diffuse nitrogen and phosphorus pollution in a medium-sized watershed, southeast China. *Estuarine, Coastal and Shelf Science* 86:387–394
- Huber D (1992) Remedial action plan—Wheatley Harbour stage 1 report. Ontario Ministry of Environment and Energy, Environment Canada, Ontario Ministry of Natural Resources and Ontario Ministry of Agriculture and Food, Ontario
- Illinois Department of Natural Resources (2009) Fish assemblages and stream conditions in the Fox River basin: Spatial and temporal trends 1996–2007. Division of Fisheries Report. IDNR, Plano
- Illinois State Water Survey (2009) Illinois climate normal data. <http://www.isws.illinois.edu/data/climatedb/choose.asp?stn=110338>. Accessed 23 Nov 2010

- Leon LF, Soulis ED, Kouwen N, Farquhar GJ (2002) Modelling diffuse pollution with a distributed approach. *Water Science and Technology* 45(9):149–156
- Liao H-H, Tim US (1997) An interactive modeling environment for non-point source pollution control. *Journal of the American Water Resources Association* 33(3):1–13
- LimnoTech (2010) Blanchard watershed AnnAGNPS modeling final report. Prepared for United States Corps of Engineers Buffalo District. Limno Tech, Ann Arbor
- Liu HC, Zhang LP, Zhang YZ, Hong HS, Deng HB (2008) Validation of an agricultural non-point source (AGNPS) pollution model for a catchment in the Jiulong River watershed, China. *Journal of Environmental Sciences (China)* 2(5):599–606
- Manonmani K (2010) Spatio-temporal analysis of land use in fringe area using GIS—a case study of Madurai City, Tamil Nadu. *International Journal of Geomatics and Geosciences* 1:264–270
- McDowell R, Sharpley AN, Folmar G (2001) Phosphorus export from an agricultural watershed: linking source and transport mechanisms. *Journal of Environmental Quality* 30:1587–1595
- McFarland MS, Hauck LM (2001) Determining nutrient export coefficients and source loading uncertainty using in-stream monitoring data. *Journal of the American Water Resources Association* 37(1):223–236
- Meixler MS, Bain MB (2010) A water quality model for regional stream assessment and conservation strategy development. *Environmental Management* 45:868–880
- Mudroch A (1984) Chemistry, mineralogy, and morphology of Lake Erie suspended matter. *Journal of Great Lakes Research* 10:286–298
- Mudroch A, Duncan G (1986) Distribution of metals different size fractions of sediment from the Niagara River. *Journal of Great Lakes Research* 12:117–126
- Nash JE, Sutcliffe JV (1970) River flow forecasting through conceptual models. Part 1: a discussion of principles. *Journal of Hydrology* 10(3):282–290
- National Research Council (2000) Clean coastal waters: understanding and reducing the effects of nutrient pollution. National Academy Press, Washington, DC
- Natural Resources Conservation Service (2010) Watershed planning: Blackberry Creek watershed. <http://www.il.nrcs.usda.gov/technical/engineer/blackberry.html#ResourceConcerns>. Accessed 5 Dec 2010
- Ng HYF, Xu N, Lam DCL, Wong I (1994) Simulation of non-point pollutant loads to Lake Chaohu from Nanfei–Dianbu watershed. Technical note no. 94. National Water Research Institute, Burlington
- Oloya TO, Logan TJ (1980) Phosphate desorption from soils and sediments with varying levels of extractable phosphate. *Journal of Environmental Quality* 9:526–531
- Ontario Ministry of Agriculture, Food and Rural Affairs (1994) Nutrient management. Best management practices series. Queen's Printer for Ontario, Toronto
- Ontario Ministry of Agriculture, Food and Rural Affairs (2004) Metadata for soil survey complex for Ontario. <http://www.appliometadata.lrc.gov.on.ca/geonetwork/srv/en/main.home>. Accessed 3 Oct 2011
- Ontario Ministry of Natural Resources (2006) Provincial DEM v200, 10 m Resolution UTM Zone 17, Land Information Ontario Geospatial Warehouse. <http://www.applio.lrc.gov.on.ca/lids>. Accessed 31 May 2010
- Ontario Ministry of Natural Resources (2010) Land Information Ontario Geospatial Warehouse. <http://www.applio.lrc.gov.on.ca/lids>. Accessed 31 May 2010
- Overcash MR, Davidson JM (1989) Environmental impact of nonpoint source pollution. Ann Arbor Science Publishers, Ann Arbor
- Parajuli PB, Nelson NO, Frees LD, Mankin KR (2009) Comparison of AnnAGNPS and SWAT model simulation results in USDA–CEAP agricultural watersheds in south-central Kansas. *Hydrological Processes* 23:748–763
- Praskievicz S, Chang H (2011) Impacts of climate change and urban development on water resources in the Tualatin River Basin, Oregon. *Annals of the Association of American Geographers* 101(2):249–271
- Randhir TO, Hawes AG (2009) Watershed land use and aquatic ecosystem response: ecohydrologic approach to conservation policy. *Journal of Hydrology* 364:182–199
- Rudra R, Dickinson WT, Clark DJ, Wal GJ (1986) GAMES—a screening model of soil erosion and fluvial sedimentation in agricultural watersheds. *Canadian Water Resources Journal* 11(4):58–71
- Schlesinger WH (1991) Biogeochemistry: analysis of global change. Academic Press, Toronto
- Sharpley AN (1995) Identifying sites vulnerable to phosphorus loss in agricultural runoff. *Journal of Environmental Quality* 24: 947–951
- Sharpley AN, Menzel RG (1987) The impact of soil and fertilizer phosphorus loss on the environment. *Advances in Agronomy* 41:297–324
- Sharpley AN, Smith SJ, Jones OR (1992) The transport of bioavailable phosphorus in agricultural runoff. *Journal of Environmental Quality* 21:30–35
- Sharpley AN, Daniel T, Sims T, Lemunyon J, Stevens R, Parry R (2003) Agricultural phosphorus and eutrophication second edition. Agricultural Research Service Paper Publication ARS-149. United States Department of Agriculture
- Shen Z, Hong Q, Yu H, Niu J (2010) Parameter uncertainty analysis of non-point source pollution from different land use types. *Science of the Total Environment* 408:1971–1978
- Shen Z, Hong Q, Chu Z, Gong Y (2011) A framework for priority non-point source area identification and load estimation integrated with APPI and PLOAD model in Fujiang Watershed, China. *Agricultural Water Management* 98:977–989
- Singh J, Knapp HV, Arnold JG, Demissie M (2005) Hydrological modeling of the Iroquois River watershed using HSPF and SWAT. *Journal of the American Water Resource Association* 41:343–360
- Soil Conservation Service (1968) Engineering handbook: supplement A to section 4. USDS–SCS, Washington, DC
- Srinivasan MS, McDowell RW (2009) Identifying critical source areas for water quality: 1. Mapping and validating transport areas in three headwater catchments in Otago, New Zealand. *Journal of Hydrology* 379:54–67
- Sugiharto T, McIntosh TH, Uhrig RC, Lardinois JJ (1994) Modeling alternatives to reduce dairy farm and watershed nonpoint source pollution. *Journal of Environmental Quality* 23:18–24
- The Conference Board of Canada (2010) Environment: water quality index. <http://www.conferenceboard.ca/hcp/details/environment/water-quality-index.aspx#Canada>. Accessed 15 April 2010
- Thompson A, Prokopy LS (2009) Tracking urban sprawl: using spatial data to inform farmland preservation policy. *Landuse Policy* 26:194–202
- Turner LJ (1994) ²¹⁰Pb dating of sediments from Malden Creek (core 053) and Muddy Creek (core 054). Technical note RAB-TN-93-Y3. National Water Research Institute, Burlington
- United States Census Bureau (2010) State and county quick facts. <http://quickfacts.census.gov/qfd/states/17/17089.html>. Accessed 10 Dec 2010
- United States Department of Agriculture (2009) Agricultural systems overview. <http://www.nifa.usda.gov/fo/sustainableagroecosystems/scienceagri.cfm?pg=3>. Accessed 15 April 2010
- United States Environmental Protection Agency (2002) National water quality inventory: 2002 report to Congress. USEPA, Office of Water Regulations and Standards, Washington, DC

- Wang X, Hao F, Cheng H, Yang S, Zhang X, Bu Q (2011) Estimating non-point source pollutant loads for the large scale basin of the Yangtze River in China. *Environmental Earth Sciences* 63(5): 1079–1092
- Wu S, Li J, Huang G (2005) GIS applications to agricultural non-point source pollution modeling: a status review. *Environmental Informatics Archives* 3:202–206
- Young RA, Onstad CA, Bosch DD, Anderson WP (1994) AGNPS, agricultural nonpoint source pollution model, version 5.00: AGNPS user's guide. USDA–NRS–NSL, Oxford